Role of AMPK during early embryonic development of *Drosophila*

A Thesis

submitted to

Indian Institute of Science Education and Research Pune in partial fulfilment of the requirements for the BS-MS Dual Degree Programme

by

Salima Shiju

Indian Institute of Science Education and Research Pune

Dr. Homi Bhabha Road,

Pashan, Pune 411008, INDIA.

April, 2024

Supervisor: Prof. Annapoorni Rangarajan

IISC Bangalore

Certificate

This is to certify that this dissertation entitled ‘Role of AMPK during early embryonic development of *Drosophila*’ towards the partial fulfilment of the BS-MS dual degree programme at the Indian Institute of Science Education and Research, Pune represents study/work carried out by Salima Shiju at Indian Institute of Science, Bangalore under the supervision of Prof. Annapoorni Rangarajan, Developmental biology and Genetics Department and at IISER Pune under the supervision of Prof. Richa Rikhy, Department of Biology in the year 2023-2024.

Prof. Annapoorni Rangarajan

Committee:

Prof. Annapoorni Rangarajan

Prof. Richa Rikhy

Declaration

I hereby declare that the matter embodied in the report entitled " Role of AMPK during early embryonic development of *Drosophila*" are the results of the work carried out by me at the Development and Biological Sciences Department, Indian Institute of Science Bangalore and in affiliation with the Department of Biology , Indian Institute of Science Education & Research (IISER) Pune, under the supervision of Prof. Annapoorni Rangarajan and the same has not been submitted elsewhere for any other degree. Wherever others contribute, every effort is made to indicate this clearly, with due reference to the literature and acknowledgement of collaborative research and discussions.

Salima Shiju

20191227

This thesis is lovingly dedicated to the imminent arrival of Joyce's baby, a joyous event that fills our hearts with anticipation and warmth.

Acknowledgment

I express my sincere gratitude to my MS thesis supervisor, Prof. Annapoorni Rangarajan, for her exceptional mentorship. She has been incredibly supportive, approachable, and encouraging throughout my thesis work, allowing me the freedom to plan, execute, and interpret my experiments.

I am deeply thankful to my mentor, Dymphna Joyce, a PhD student in the lab, who patiently taught me fundamental embryo experimental techniques with care and affection. She has become like a sister to me, and I eagerly anticipate the arrival of her baby.

I extend my heartfelt appreciation to Prof. Richa Rikhy from IISER, Pune, who graciously guided me through challenging experiments and provided invaluable advice and suggestions.

I am grateful to all members of Prof. Annapoorni Rangarajan's lab, particularly Girish and Malavika, for fostering a positive, fun and supportive research environment. This lab provided a nurturing space for students to explore various research areas, with senior members always willing to assist and teach, even for the most basic queries.

I am indebted to the microscopy and fly facilities at IISC and IISER Pune, whose seamless operation facilitated the completion of my MS project.

Special thanks to the members of Richa lab, especially Aparna, for their assistance, advice, and willingness to share resources. I would also like to express my gratitude to Subhradip from Prof. Girish Ratnaparki's Lab for guiding me through certain experiments.

My heartfelt thanks go to my family (achan, amma, chechi, kunchu, and my cousins) and friends (too numerous to name individually) for their unwavering support, patient listening, and keeping me grounded throughout my endeavours.

Finally, I acknowledge and thank myself for persevering through challenges and emerging stronger and more motivated each time.

LIST OF ABBREVIATIONS USED

NG4	*nanos*-Gal4
DaG4	*daughterless*-Gal4
NC	Nuclear Cycle
AMPK^{i}	UAS- AMPK RNA^{i}
Ortho	Orthogonal
MZT	Maternal to Zygotic Transition
pAMPK	phosphorylated AMPK
tAMPK	total AMPK
Dlg	Discs large

Table of Contents

LIST OF FIGURES

LIST OF TABLES

Abstract

AMP-activated protein kinase (AMPK) is an energy sensor that regulates cellular metabolism. In *Drosophila melanogaster*, mono-allelic expression of AMPK-α, -β, and -γ yields a single heterotrimeric energy sensor. Functionally critical amino acids of AMPK subunits and upstream kinases are conserved across humans and *Drosophila*. All this collectively makes *Drosophila* an ideal model system where the function of AMPK has been fairly less explored in embryonic stages. During syncytial blastoderm formation and cellularization, the embryo undergoes intricate changes including furrow extension, maintenance of the actomyosin network to facilitate contractile ring constriction, and establishment of polarity markers such as Dlg to ensure normal cellular growth. This study aims to elucidate the role of AMPK during both the syncytial blastoderm stage and the subsequent cellularization stage of *Drosophila* embryonic development. Our focus lies on investigating the dynamic localization patterns of AMPK and how they differ from those observed in mammalian systems. Furthermore, we seek to understand how AMPK contributes to the regulation of membrane organization during these critical developmental stages.

CHAPTER 1 INTRODUCTION

Drosophila melanogaster, commonly known as the fruit fly, is a holometabolous insect that undergoes an orchestrated life cycle of four distinct stages: embryo, larva, pupa, and adult. The journey begins with the fertilization of an egg, giving rise to a 0.5 mm long embryo that hatches within a short period of 12 to 15 hours, initiating the larval phase. The larval stage, further delineated into three instars—first, second, and third—marks a period of rapid growth and formation of undifferentiated sacs of cells called imaginal discs. Notably, around the fourth day, during the third instar larval stage, the larva transitions into the crawling stage. Following this, the larva undergoes encapsulation to form a puparium, where it undergoes metamorphosis in which most larval tissues get degraded while specialized precursor cells known as imaginal discs orchestrate the emergence of distinct adult structures.

Remarkably, the entire life cycle of *Drosophila melanogaster* is completed within a mere ten days at room temperature. Moreover, the *Drosophila* genome, comprising four pairs of chromosomes (X/Y, II, III, and IV), with the majority of genes located on chromosomes X, II, and III, this species boasts approximately 15,000 protein-coding genes—half the number found in the human genome. The combination of its short generation time, well-sequenced genome, ease of maintenance in laboratory conditions, and high fecundity renders *Drosophila melanogaster* an indispensable tool for elucidating fundamental principles in genetics, developmental biology, and beyond.

1.1 *Drosophila* embryogenesis

During *Drosophila* embryogenesis, a distinctive pattern of rapid synchronous nuclear cycles characterizes early development. These cycles consist of S and M phases, occurring without cytokinesis for approximately nine cycles, each lasting around 8 minutes, at the center of the zygote. This results in forming a syncytial blastoderm comprising 256 nuclei sharing a common cytoplasm. Around nuclear cycle 10, these nuclei commence migration towards the cytoplasm's periphery during interphase (Rabinowitz, 1941). Nuclear cycles 11-13 occur at the periphery of the syncytial blastoderm. During this period, despite the absence of plasma membrane boundaries, there is a designated nucleo-cytoplasmic region for each nucleus with their organelles and restricted motion of microtubules in between this nucleo-cytoplasmic region (Frescas et al., 2006). Subsequently, the cell cycle gradually slows down, with interphase stages lengthening. Notably, during cycle 14, around 150 to 180 minutes after the onset of the cycle, a significant transformation occurs during the extended S phase. Cell membranes of approximately 3 to 5 micrometre length begin to extend into the cytoplasm around each of the approximately 6000 nuclei, marking the onset of cellularization forming a

cortical layer of epithelial cells. The actomyosin contractile structures are present at the ingressing membrane fronts which regulate the membrane extension (He et al., 2016). Following this stage, the first Gap 2 phase (G2) ensues, accompanied by gastrulation, which takes around 180 to 240 minutes, characterized by the invagination of mesodermal precursors to form the ventral furrow and the formation of the cephalic furrow (Foe et al., 1989; Edgar et al., 1989). Cell cycle speed is a consequence that helps in cellularisation and gastrulation by having elongated S phase and G2 phases to conduct morphogenesis (Seher et al., 2000).

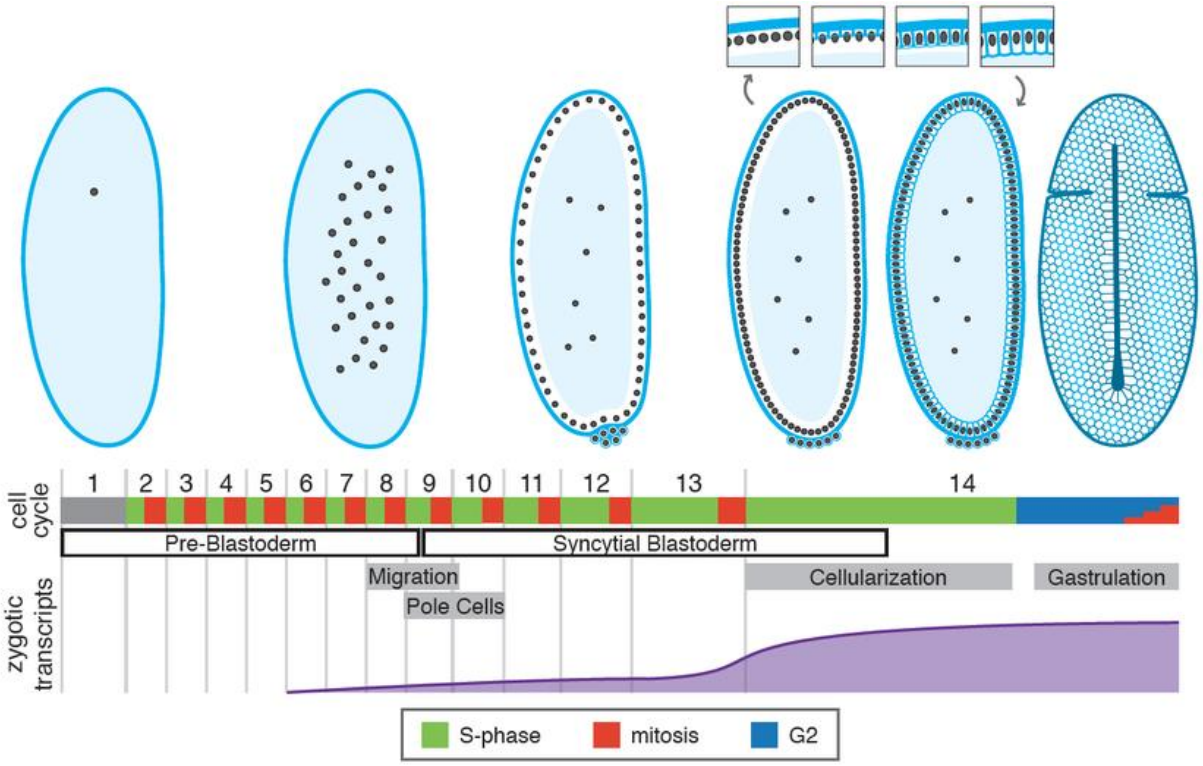

Fig 1.1 Early embryonic development in *Drosophila*. The diagram illustrates the initial 14 cycles of Drosophila development, highlighting key morphological stages. While most embryos are depicted in cross-section with the ventral side to the right, the final illustration shows a surface view with the ventral side facing upward. Cellularization is depicted in more detail in insets. The duration of S phase, mitosis, and G2 phase is indicated by color-coding: green for S phase, red for mitosis, and blue for G2 phase. Mitosis 14 is depicted as a series of small bars due to the embryo becoming asynchronous, with different cell groups entering mitosis at varied times according to developmental programming. Notable morphological events, such as nuclear migration to the blastoderm and the cellularization of pole cells to insulate the germline, are marked in grey boxes. Additionally, the onset of ventral furrow formation, representing the first gastrulation movement, is highlighted. Below the diagram, the approximate number of genes with detected zygotic transcripts over time is presented (Jeffery et al., 2014).

1.2 Maternal-to-Zygotic Transition

During the initial stages of embryogenesis, the zygotic genome remains inactive, and maternal transcripts direct cellular processes. In *Drosophila*, a substantial portion of the genome, approximately 55–65%, is contributed maternally as RNA (Lott SE et al., 2011; Foe et al., 2017). The spatial and temporal expression patterns of these maternal transcripts play a

crucial role in the developmental patterning of the embryo. As the embryo progresses, around cell cycle 14, the activation of the zygotic genome becomes vital for regulating embryonic development (Palfy et al., 2017). This transition is known as maternal to zygotic transition (MZT). Hence, the initial stages of embryonic development are governed by maternal transcripts. MZT is regulated by the combined activity of maternal and zygotic-driven RNA decay mechanisms, ensuring the gradual elimination of maternally deposited transcripts during this critical period (Bashirullah et al., 1999).

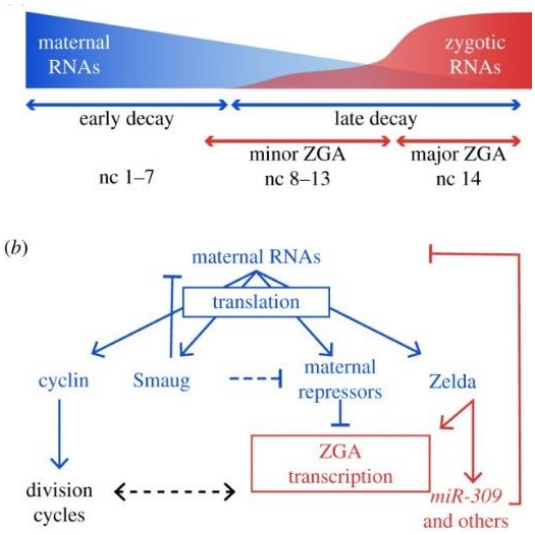

Fig 1.2 MZT in *Drosophila*. During the maternal-to-zygotic transition (MZT), there is a model of maternal and zygotic gene expression dynamics. Maternal mRNA stores undergo degradation through two RNA degradation pathways: an 'early decay' pathway initiated by maternally provided factors post-egg activation, independent of zygotic transcription, and a 'late decay' pathway mediated by factors expressed by the zygote. Zygotic genome activation (ZGA) unfolds gradually over the MZT. Initially, there is the early onset expression of approximately one hundred zygotic genes, known as minor ZGA, occurring several nuclear cycles before the subsequent widespread activation of the zygotic genome, referred to as major ZGA (Hamm et al., 2018).

1.3 AMPK- structure, regulation, and function

Adenosine monophosphate-activated protein kinase (AMPK) serves as a pivotal protein kinase in the cascade pathway that governs energy homeostasis. It comprises three subunits: α (a catalytic subunit), β, and γ (regulatory subunits). AMPK undergoes allosteric activation when the Thr172 site of the alpha subunit is phosphorylated by upstream kinases such as LKB1, CAMKKβ and TAK1 resulting in the formation of pAMPK (Hardie, 2004). This activation is finely tuned in response to energy stress, particularly when the AMP:ATP ratio increases (Gowans et al., 2013). CAMKKβ is another upstream kinase of AMPK, which phosphorylates the conserved threonine site by increased calcium flux and calmodulin in response to any hormone, stress, or drug (Cantrell, 2019). TGF-β and pro-inflammatory cytokines activate TAK1 mediated phosphorylation of AMPK. Several studies prove that cellular ROS (reactive

oxygen species) and glucose deprivation are also capable of AMPK activation (Neumann, 2018). Conversely, if the AMP:ATP ratio is maintained, AMPK is dephosphorylated by phosphatases like PP2A, PP2C, and PP1. Autophosphorylation at specific threonine and serine sites by Akt, DAG, and PKA causes blockage of upstream kinases from phosphorylating (Hawley et al., 2014). Ubiquitination by some proteins inhibit the activity of AMPK by its degradation (Vila et al., 2017).

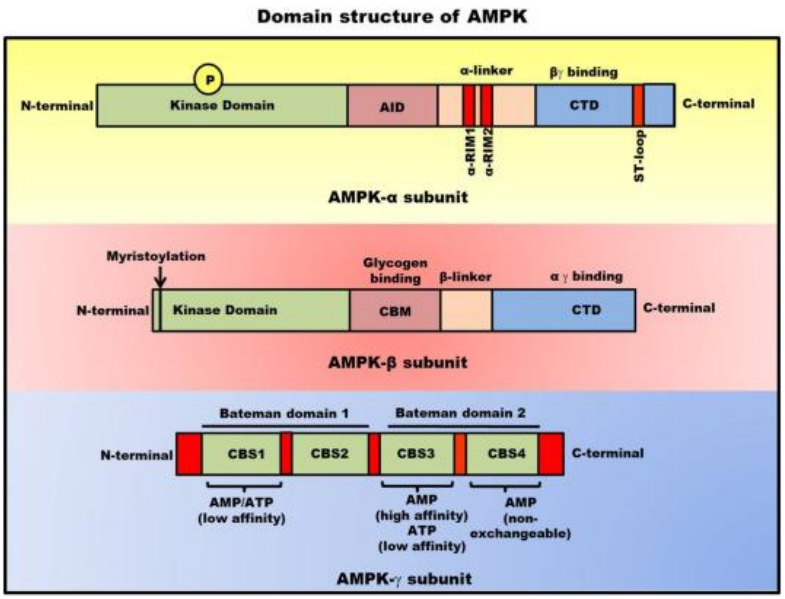

Fig 1.3 Domains and structure of the AMPK complex. The AMPK trimeric complex comprises a catalytic subunit (α) and two regulatory subunits (β and γ). The key domains of AMPK are depicted here. These include the carbohydrate-binding module (CBM), cystathionine β-synthase repeats (CBS), N terminus domain (NTD), C terminus domain (CTD), autoinhibitory domain (AID), serine/threonine-enriched loop (ST-loop), and regulatory-subunit-interacting motif (RIM) (Sharma et al., 2023).

AMPK serves as an energy sensor through its four cystathionine β-synthase repeats (CBS) present on γ subunit, which competitively bind to AMP, ADP, and ATP (Gowans et al., 2013). During periods of high AMP:ATP ratio, AMPK restores energy balance by inhibiting anabolic processes such as fatty acid synthesis via phosphorylation of ACC1, protein synthesis via phosphorylation of TSC2 which inhibits m-TORC1, glycogen synthesis via phosphorylation of glycogen synthase, rRNA synthesis via phosphorylation of TIF-1A, etc, which consume ATP. Simultaneously, it promotes catabolic processes like glycolysis, glucose uptake, increased TCA cycles and mitochondrial biogenesis via upregulation of PGC-1- α, fatty acid oxidation via phosphorylation of ACC2, mitochondrial fission via phosphorylation of ULK1 which generates ATP (Ciruelos et al., 2020). The structural arrangement of AMPK ensures that the phosphorylation and dephosphorylation of Thr172 are sensitive to conformational rearrangements induced by nucleotide binding. Therefore, mammalian AMPK activation by AMP occurs through a tripartite mechanism: 1) promotion of Thr172 phosphorylation; 2) inhibition of Thr172 dephosphorylation; 3) allosteric activation (Sharma et al., 2023). Hence, the canonical function of the AMPK pathway is to regulate the integrated signaling network, which plays a major role in regulating cellular metabolic processes.

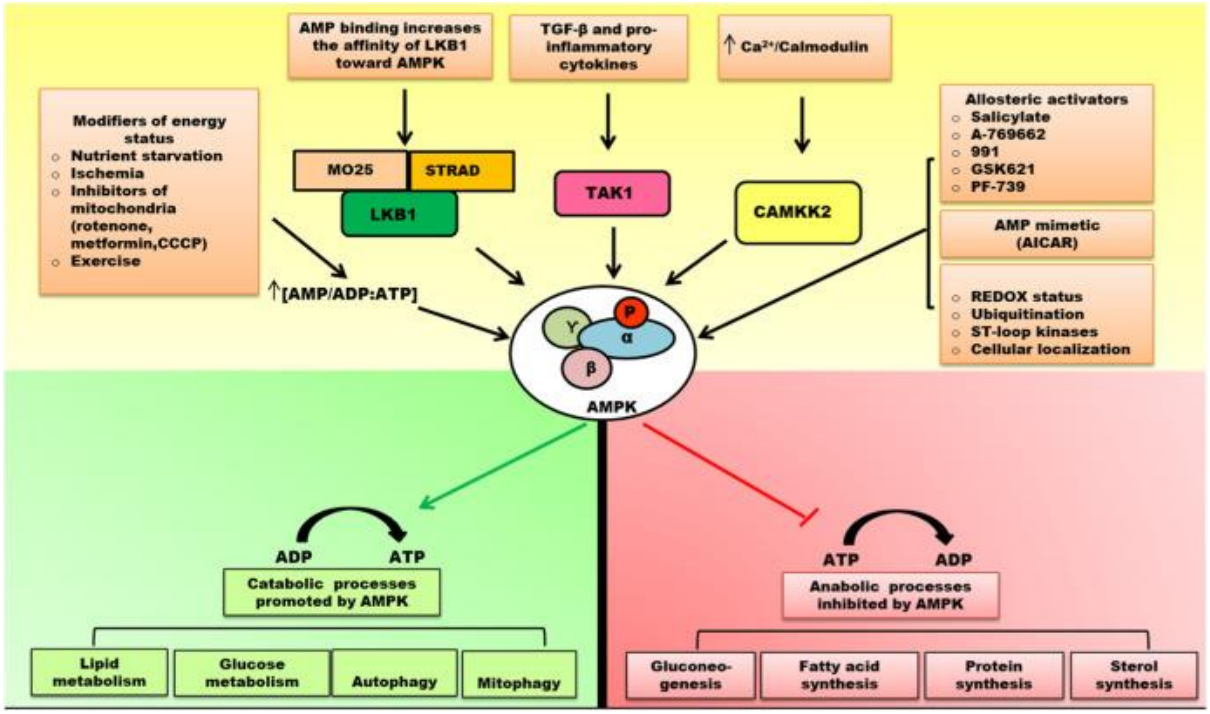

Fig 1.4 AMPK activation via upstream kinases, nucleotides, pharmacological agents and its downstream effects.

The kinases upstream of AMPK, including liver kinase B1 (LKB1), TAK1, and CAMKK2, are depicted above the AMPK complex. The LKB1 heterotrimeric complex, consisting of LKB1, STRAD, and MO25, activates AMPK upon binding to AMP. TAK1 is activated by factors such as TGF-β and pro-inflammatory cytokines, while CAMKK2 is activated by intracellular calcium and calmodulin. Additionally, AMPK can be activated by various stimuli, such as glucose starvation, exercise, and mitochondrial poisons. AMP mimetic AICAR and various small-molecule allosteric activators are also effective in activating AMPK. Upon activation, AMPK helps maintain energy balance by decreasing ATP-consuming anabolic processes and increasing ATP-generating catabolic processes in response to disturbances in cellular AMP/ADP:ATP ratio (Sharma et al., 2023).

1.4 AMPK as tumor suppressor

LKB1, belonging to the tumor suppressor gene family, crucially regulates AMPK, its downstream target. Loss of LKB1 function disrupts various cellular processes in human tumor cells, including biosynthesis control and cell cycle progression, leading to reduced cell growth and proliferation (Hawley et al., 2003). LKB1 has also showed its regulation on epithelial cell polarity in drosphila and mammals. AMPK has emerged as a significant tumor suppressor, evident in studies where its complete genetic loss in B and T cell lymphoma cells accelerates tumor initiation. Its ability to inhibit mTORC1 and curb protein synthesis for enhanced ATP production is particularly noteworthy, as mTORC1 is commonly upregulated in cancer (Ji et al., 2007). Metformin, an AMPK activator, in type 2 diabetes treatment has shown promise in reducing cancer risk, further highlighting AMPK's potential in cancer prevention and treatment (Noto et al., 2012). However, AMPK is just one of twelve AMPK-related kinases (ARKs) downstream of LKB1. Therefore, while AMPK plays a significant role in mediating LKB1's tumor suppressor function, other LKB1/ARK-mediated pathways may also contribute to this

tumor suppressor function (Jaleel et al., 2005; Lizcano et al., 2004). There are reports showing pharmacological activators of AMPK suppress tumor cell functions (Fogarty et al., 2016). Studies on ubiquitin ligases, which are involved in the degradation of AMPK subunits, also supported the idea of AMPK as a tumor suppressor (Pineda et al., 2015; Vila et al., 2017).

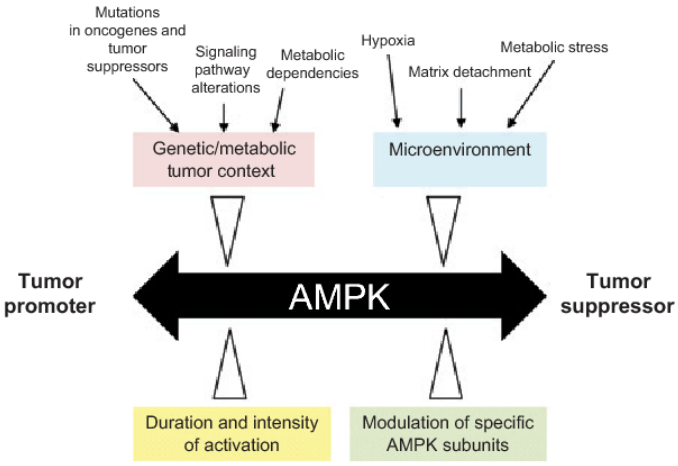

Fig 1.5 AMPK functions as tumor suppressor and tumor promoter. The impact of AMPK activation in cancer is influenced by various factors including the genetic makeup of the tumor cells, their metabolic requirements, and the surrounding tissue environment. Variances in the level and duration of AMPK activation, such as natural physiological activation versus artificially induced high-level activation through drugs, along with variations in the expression and activation of specific subunits within the AMPK heterotrimer, play a significant role in determining whether AMPK acts as an inhibitor or promoter of tumor growth across different types of cancer (Zadra et al., 2015).

1.5 AMPK as a tumor promoter

Conversely, AMPK can promote cancer by protecting tumor cells against pathological/physiological stresses like nutrient deprivation, hypoxia, and matrix detachment, associated with the progression of the tumor (Jeon et al., 2012). Studies have proven pro-tumorigenic functions for AMPK promoting anchorage-independent growth, inhibition of apoptosis, cancer cell migration, and invasion potential, and induction of EMT as well as the maintenance of EMT phenotype (Liang et al., 2013). During metastasis, when the tumor cells get detached from primary tumor sites and enter the circulation as circulatory tumor cells (CTC), they hijack EMT, an evolutionarily conserved developmental program (Yang et al., 2006). AMPK activation leads to EMT. Indeed, some studies show re-attachment to the matrix by exhibiting epithelial properties over mesenchymal properties named MET, which downmodulates AMPK, indicating at later stages AMPK might be inactivated (Saxena et al., 2018). EMT-derived tumor cells confer enhanced mobility, invasion, and resistance to apoptotic stimuli as well as stem cell properties, helping them exhibit therapeutic resistance (Polyak and Weinberg, 2009). AMPK has a direct role in the induction of EMT in cancer cells and its maintenance, which is mediated by physiological cues like hypoxia and TGFβ via HIF-

1α (Tam et al., 2020). This regulation of AMPK on EMT is via upregulation of the TWIST1 gene and its nuclear localisation (Saxena et al., 2018).

1.6 Non-canonical role of AMPK

AMPK's role extends beyond energy regulation; it also governs cell cycle checkpoints in cancer cells to modulate proliferation in response to stress (Mihaylova and Shaw, 2011). Mitotic failure can lead to errors in developmental processes and tumor initiation. In *Drosophila*, AMPK null germline clone mutants exhibit embryonic lethality, highlighting its crucial role in development (Lee et al., 2007). In addition to its canonical functions, AMPK has non-canonical roles in mitotic regulation and epithelial polarity. It phosphorylates MRLC(myosin regulatory light chain), which is a critical molecule for mitosis and cell polarity in both mammals and *Drosophila* (Thaiparambil et al., 2012). In AMPK mutants, because of loss of active MRLC, disorganisation in epithelial structure, abnormal genomic integrity, defective mitotic cells (polyploid chromosome) and abnormal cell polarity were observed (Thaiparambil et al., 2012). AMPK also regulates mitotic spindle orientation, with active AMPK (pAMPK) dynamically localizing along spindle poles. Mutant forms of AMPK can cause misorientation of spindle poles, leading to mitotic delays (Lu et al., 2021). A chemical genetic screen of AMPK subunits revealed multiple mitotic genes targeted by AMPK phosphorylation (Banko et al., 2011). Furthermore, CDK1 has been identified as an essential upstream kinase for AMPK determined by PLK1, regulating cell entry into mitosis and genomic stability (Lu et al., 2021). These studies underscore AMPK's role as a master regulator of cell cycle progression, with implications for both normal development and cancer. AMPK activation also helps in the formation of epithelial cell junction assembly and its maintenance. AMPK regulated this through ZO-1/afadin localisation during the junction assembly (Wu et al., 2020). Studies on MDCK cells show the mechanism through which AMPK regulated epithelia tight

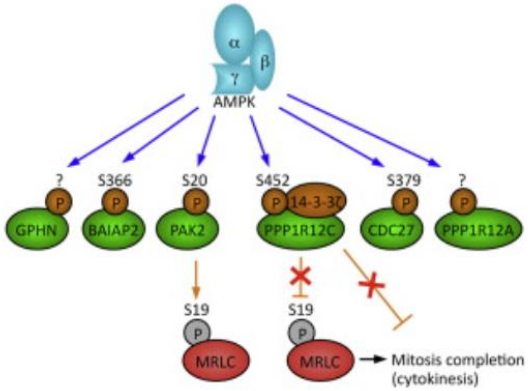

Fig 1.6 AMPK regulate mitosis. AMPK directly phosphorylates a number of substrates involved in coordinating different aspects of mitosis. Chemical Genetic Screen for AMPKα2 Substrates Uncovers a Network of Proteins Involved in Mitosis (Banko et al., 2011).

junction assembly and disassembly depending on the cellular energy status and calcium level (Zheng et al., 2006). AMPK has also seen to regulate and reorganise actin cytoskeleton, predominantly F-actin for cell polarity, cell migration and cell division through osmotic stress and calcium level (Miranda et al., 2010). AMPK activation by pharmacological and genetic inhibition of ATP production by mitochondria has been shown to decrease syncytial metaphase furrow extension (Chowdhary et al., 2017).

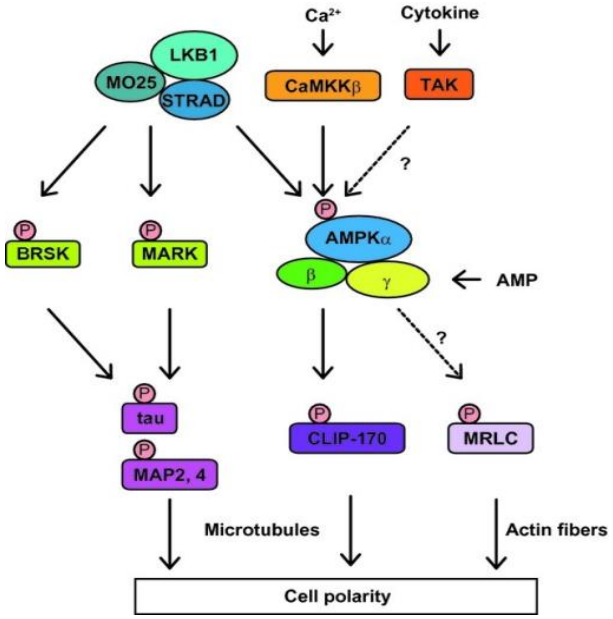

Fig 1.7 AMPK signaling pathways related to cell polarity. The trimeric complex composed of LKB1, STRAD (STe20-Related ADaptor), and MO25 directly phosphorylates and activates BRSK, microtubule affinity-regulating kinase (MARK), and AMPK, all of which are protein kinases related to AMPK. AMPK is activated through direct binding of AMP to its γ subunit, thereby reflecting the cellular energy status. Additionally, AMPK can be phosphorylated by CaMMKβ in response to elevated intracellular calcium levels. The phosphorylation of tau, MAP2, and MAP4 by activated BRSK and MARK, as well as the phosphorylation of CLIP-170 by AMPK, play roles in regulating cell polarity through modulation of microtubule dynamics. The dashed line with a question mark represents a pathway that necessitates further investigation. MAP refers to microtubule-associated proteins (Nakano et al., 2012).

1.7 Why *Drosophila* and AMPK?

Drosophila serves as an advantageous model for investigating the role of AMPK due to its conserved signalling pathways, which exhibit a level of complexity akin to mammals but with more straightforward genetic approaches. The monoallelic expression of AMPK subunits -α, -β, and -γ in *Drosophila* results in the formation of a single AMPK heterotrimer, simplifying genetic studies compared to mammals, where multiple isoforms of each subunit (α1–2, β1–2, and γ1–3) are encoded (Iseli et al., 2005; Pan and Hardie, 2002). This streamlined genome facilitates gain-of-function and loss-of-function studies in vivo., Furthermore, functionally critical amino acids that regulate AMPK localization, subunit interactions, and activity, as well as upstream kinases like LKB1 and AMPK substrates like ACC, are conserved across species or replaced by biochemically similar residues (Chen et al., 2012; Kazgan et al., 2010; Pan and Hardie, 2002). This conservation allows researchers to translate findings from *Drosophila* to mammalian systems. Additionally, *Drosophila* geneticists benefit from a vast array of toolkits, including P-elements, the Gal4-UAS system, transgenic RNAi approaches, and high-throughput screening methods. These tools provide powerful means for manipulating gene expression and conducting large-scale genetic screens, enabling comprehensive studies of AMPK function and regulation in vivo (Sinnet et al., 2016).

Investigating the role of AMPK during various stages of early embryonic development in *Drosophila* remains a relatively unexplored area of research. However, understanding AMPK's function in these stages could provide valuable insights into its regulation of cell cycle progression, particularly in the context of the rapid synchronous mitotic divisions that characterize early *Drosophila* embryo development. By examining AMPK's role in this process, researchers can elucidate its control over chromosome stability and its localization throughout different stages of the cell cycle. Moreover, studying AMPK's impact on membrane organization during embryonic development, including processes such as syncytial blastoderm, cellularization and early gastrulation, can provide insights into AMPK's broader role in regulating cellular structure and organization during embryogenesis.

Additionally, investigating the effect of AMPK knockdown on the epithelial-mesenchymal transition (EMT) process during ventral invagination of presumptive mesoderm can shed light on AMPK's involvement in this critical developmental process. Understanding how AMPK influences EMT during development may provide insights into its potential role in cancer metastasis, as EMT is also a key event in tumor progression. Furthermore, considering the well-studied role of Twist during development and its connection to cancer, exploring the regulation of Twist by AMPK during EMT could provide valuable insights into how cancer hijacks developmental processes for its benefit. Investigating whether Twist is a downstream substrate for AMPK during EMT and how this regulation impacts cellular behavior could deepen our understanding of the molecular mechanisms underlying cancer progression and potentially identify new therapeutic targets.

CHAPTER 2 Materials and Methods

2.1 *Drosophila melanogaster* genetics

All fly lines were grown at 25^{o}C using standard 6% fly media. The composition of 6% fly media consists of 6% w/v malt, 7.5% w/v corn flour, 1% w/v agar, 1.5% w/v yeast, 8% w/v sugar, 0.5% v/v propionic acid, 0.1% v/v orthophosphoric acid, 0.07% w/v methylparaben and 0.5% v/v ethanol in water. The fly bottles for virgin isolation were kept in a 25^{o}C incubator, and the virgins were collected in vials with 3% fly media. The collected virgin flies were then used for cross-setup within 5 days of collection to ensure they were not overly aged. The lines used for this study are mentioned in the table

Name	BDSC ID	Genotype and comment
CS	-	Canton-S, from Richa Rikhy's lab at IISER Pune. Used as control in all experiments by crossing to mat67
Da Gal4	27608	w[*];P{w[+mC]=UAS-NLS-V5-TEV-NLS2}3,P{w[+mW.hs]=GAL4 da.G32}UH1/TM3, Sb[1] Ubiquitous expression of GAL4 under the control of daughterless.
nanos-Gal4	-	Lab stock (Mavrakis et al., 2009; Mavrakis et al., 2008)
AMPKi	32371	y[1]sc[*] v[1]sev[21]; P{y[+t7.7] v[+t1.8]=TRiP.HMS00362}attP2 UAS (regulatory), AMPKalpha (RNAi) Expresses dsRNA for RNAi of AMPKalpha (FBgn0023169) under UAS control in the VALIUM20 vector.
Histone EGFP	24163	w[*]; P{w[+mC]=His2Av-EGFP.C}2/SM6a Expresses a EGFP-tagged Histone H2A variant in all cells.
tGPH	8163	w[118]; P{w[+mC]=tGPH}2; Sb[1]/TM3, Ser[1] Expresses a fusion protein composed of GFP and the pleckstrin homology domain of Grp1 under the control of the alphaTub84B promoter; localizes to plasma membrane in the presence of phosphatidylinositol-3,4,5-trisphosphate (PIP3).
UAS GFP	1521	w[*]; P{w[+mC]=UAS-GFP.S65T}Myo31DF[T2] Expresses GFP.S65T under the control of UAS.

Table 2.1 All the information in this table is sourced from the official website of the Bloomington Drosophila Stock Center (BDSC) and from FlyBase.

2.2 Crosses

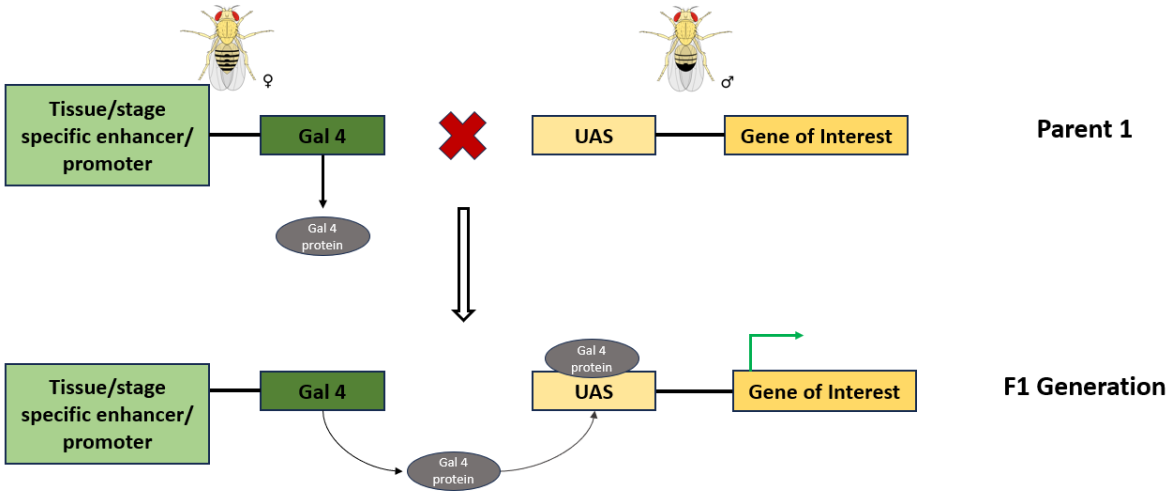

Fig 2.1 GAl 4-UAS system in *Drosophila*. A fly bearing a gene X downstream of a UAS enhancer sequence is crossed to another fly bearing a GAL4 gene downstream of a tissue Y-specific promoter. The F1 flies produce GAL4 restricted to tissue Y, and the GAL4 binds to the UAS sequence and activates the expression of gene X within tissue Y.

nanos-Gal4 was used to induce stage-specific expression during oogenesis and early stages of embryo development. To confirm the specificity of the Nanos Gal4 driver line used, UAS GFP is crossed with it and checked from green fluorescence in the abdomen of F1 Flies and embryos laid by F1 flies under epifluorescent scope. RNAi-mediated knockdown line of AMPK, UAS-AMPK RNAi (BL #32371, AMPK alpha (RNA^i)) was used. To check the lethality of the AMPKi line used, it is crossed with Da Gal4, and the generation of F1 progeny is analysed. Histone GFP Nanos Gal4 and tGPH PIP3 maternal tubulin gal 4 lines are crossed with the UAS-AMPK RNAi line for live imaging. To generate the Histone GFP Nanos Gal4 line, the Histone GFP/Histone GFP line is crossed with the Nanos Gal4/Nanos Gal4 line and maintained at 25oC, and the F1 virgins from this cross are made to cross with the UAS AMPKi line. 2 to 3 replicates of each cross were made in bottles with 6% fly media and maintained at 28^{o}C. The Nanos Gal4 virgins collected are crossed with Canton S males as a control cross.

The cross-setup bottles were flipped every third day, and the resulting F1 flies were transferred to cage setup for embryo collection. The egg-laying plates of the cage are made of 2.5% w/v agar and 3% w/v sucrose plates smeared with fresh yeast paste. These cages were maintained at the same temperature as the parent crosses corresponding are maintained and were acclimatised for 2 days. The F2 embryos collected on the plate is later used for experiments.

2.3 Embryo Viability Assay

Freshly hatched females and males from the F1 generation of the experimental cross (Nanos-Gal4 * UAS AMPK RNA^i) and control cross (CS * UAS AMPK RNA^i) were acclimatized in an embryo collection cage for two days to prepare for embryo harvest. The plates were discarded and a fresh plate was attached. After 3 to 4 hours of embryo laying, embryos from the plates were arranged on a fresh plate and kept in a humid chamber (wet tissue in a 90 mm petri dish) at 29^{o}C for 24 hours. The hatched and unhatched embryos were manually counted using a stereoscope after 24 hours.

2.4 Embryo Laying Assay

Freshly hatched 30 females and 10 males from the F1 generation of the experimental cross (NanosGal4 * UAS AMPK RNA^i) and control cross (CS * UAS AMPK RNA^i) were transferred to an embryo collection cage and kept at 29oC. 2 to 3 replicates for the same was made. The plate had a thin generous layer of yeast. The number of embryos was manually counted after 6 hours for one set of flies and after 12 hours for the other; both conditions were set up independently.

2.5 Embryo collection

From the cages maintained at 28ºC, the F2 embryos were collected at 0h- 2h/3h after egg deposition (AED) for fixed staining and 0h-1h 30 min for live imaging. The embryos were dislodged from the plate using a paintbrush, and the yeast paste on the plate was dissolved in distilled water. Later, the yeast-embryo water mixture was strained through an egg basket, leaving the embryos in the basket. The embryos were washed thoroughly with distilled water to remove any remnants of yeast left behind. The washed embryos were then immersed in 4% v/v bleach solution for 1 minute 30 sec to 2 minutes for chorion layer removal of the embryos. We can check for dechorionisation of embryos by looking at it under a stereoscope, where the dorsal appendages present on the chorion layer of embryos initially will be absent after dechorionisation. The dechorionated embryos were washed thoroughly with running distilled water till the bleach smell is reduced and taken for downstream processes corresponding to the experiment to be performed, which are live imaging, fixed staining cuticle preparation and western blotting.

2.6 Extraction of proteins from embryos for immunoblotting

The dechorionated embryos are washed thoroughly and transferred to a 1.5ul Eppendorf tubes. Add 2X SDS (100mM Tris HCl (pH 6.8), 4% SDS, 0.2% Bromophenol Blue, 20% Glycerol, 200mM β-mercaptoethanol) buffer approximately 5 times the volume of embryos and homogenise the embryos by 10 to 15 strokes with the pestle in an ice bath. Allow the foam to settle down and transfer the homogenate to one or more tubes. Heat the embryo extract to 100ºC in a heat block for 5 minutes. Later let the extract cool down on ice briefly and soin in a centrifuge for 5 minutes at 20000 rpm. Load the aliquote of supernatant into the well or it can be also stored in -20ºC for later use.

2.7 Western bloting

Samples after heating for 5 minutes at 100ºC were loaded into the wells of 10% SDS gel in equal protein concentration. The gel was run at 200 V for 1 hour for separating protiens and later transfer was done to PVDF membrane activated with methanol.after 1 hour transfer at 100V, the blot was put in 5% BSA blocking solution for 1 hour. The blot was then cut accordingly and incubated in the primary antibody (pAMPk 1:1000 and tubulin 1:1000) for overnight at 4ºC on a rocking platform. Later 3 1X TBST washes for 15 minutes each were given and incubated in the respective secondary antiboies in 1:2000 dilution for 2 hours. The blot is again washed for 3 times and developed in Gel Doc. The blots probed for tubulin was stripped using 0.5M EDTA buffer and reprobed for pAMPK.

2.8 Preparation of embryos for live imaging

After being dechorionated and washed, embryos were dried with a paper towel and carefully placed onto a chamber slide using a delicate brush. The chamber was subsequently filled with 1X PBS solution. Following this, the chamber slide was placed directly onto the microscope stage to facilitate live imaging.

2.9 Preparation of embryos for cuticle preparation assay

Embryos were collected for 0-2 hours, and the egg-laying plate was aged for 22 hours to allow the development of the cuticle. Followed by dechorionisation using 4% bleach and thoroughly washing embryos. The embryos were transferred to a scintillation vial containing 100% ethanol. I swirled the vial for some time and removed it. Later embryos were washed with 100% methanol. For devitellinisation, the methanol devitellinastion method is used. The devitellinised embryos present at the bottom were washed with methanol twice and can be stored in methanol at -20^{o}C. Embryos are placed on the slide and air-dried. Around 100 ul of 85% lactic acid is dropped on the embryos, and the coverslip is placed carefully on top. The slide is placed on the slide warmer at 55^{o}C overnight, after which the slide is properly sealed with transparent nail polish.

2.10 Fixation and devitellinisation

Washed embryos were taken for fixation. The embryos were transferred to a scintillation vial containing heptane: 8% Paraformaldehyde (PFA) in equal volume, forming a phase-separated interface where embryos are stuck and left for 20 mins on a rocking platform at room temperature. For D-cad staining, the embryos are fixed using 4% PFA with 1mM EGTA. Fixed embryos, after removing the bottom layer of PFA using a micropipette, were permeabilized using heptane for around 45 minutes at room temperature. This is followed by the devitellinisation of embryos either using the methanol or the hand devitellinisation method, depending on the antibodies and dyes used for staining. For methanol devitellinisation, we used heptane: methanol (chilled) in equal volume and vigorously shook the scintillation vial for 1 to 1:30 minutes. This led to the devitellinized embryos to the bottom of the vial and the debris in the interphase, which was discarded later. The devitellinised embryos were stored in methanol at 4^{o}C. For hand devitellisation method, the embryos were then moved onto a piece of Wattman filter paper, allowing the heptane to evaporate. Next, the embryos were transferred onto double-sided tape attached to a Petri plate by placing the filter paper against the tape. Subsequently, the filter paper was carefully removed, leaving the embryos adhered to the tape. 1X PBS solution was added to the Petri plate, and a syringe needle was utilized to gently maneuver each embryo out of its vitelline envelope while the punctured vitelline envelope

remained attached to the tape. This can be observed by noticing the shiny coat-like appearance of each embryo getting lost once it came out of the vitelline membrane after gently nudging it at one end. De-vitelline embryos were preserved in 1X PBS at 4°C for up to 24 hours.

2.11 Immunostaining

De-vitellinised embryos were washed thrice with 0.3% PBST (Triton X-100 dissolved in 1X PBS) for 10 minutes each. The embryos were then blocked using BSA (Bovine Serum Albumin with sodium azide dissolved in PBST) for 1 hour. Afetr blocking, the embryos were incubated in primary antibody (diluted in BSA) for overnight (around 14 to 16 hours) at 4^{o}C on a rocking platform. The next day, embryos are again washed with 0.3% PBST thrice for 10 minutes and followed by secondary antibody or dye incubation which is diluted in 0.3% PBST. For D-cad staining, the embryos after washes are incubated for another 2 hours in Normal Goat Serum (NGS) 1:10 dilution mixed with PBST. The secondary antibody dilutions are later made in this NGS blocking solution. The vials are covered with foil to prevent photodegradation of the fluorophore conjugated to the antibody or the dye. NOTE: Hand devitellinised embryos are used for phalloidin dye and D-cadherin staining mainly. The incubation period is around two hours on a rocking platform at room temperature. Embryos are washed thrice with 0.3% PBST for 10 minutes, during which, in the second wash, Hoechst is diluted along with PBST for nucleus staining. The antibodies and dyes and their dilutions are mentioned in the table:

Primary antibodies		
Raised against	Raised in	Dilution
phospho AMPK (pAMPK)	Rabbit	1:200
total AMPK (tAMPK)	Mouse	1:200
Tubulin (Tub)	Mouse	1:200
D-cadherin (Ecad)	Rat	1:200
Squash	Rabbit	1:500
Discs large (Dlg)	Mouse	1:100
Secondary antibodies		
Raised against	Wavelengths used	Dilution
Mouse	495nm-520nm	1:1000
Rabbit	650nm-670nm	1:1000
Rat cy3	550nm-570nm	1:1000
Fluorescently coupled dyes		
Dye	Wavelengths used	Dilution

Alexa Flour Phalloidin 488/647	495nm-518/ 650nm-688nm	1:1000
Alexa Flour Streptavidin 647	650nm-688nm	1:500
Hoechst 33258	352nm-454nm	1:1000

Table 2.2 List of antibodies used

2.12 Slide Preparation

The stained embryos are transferred to a glass slide. Excess PBST was drained out carefully using a Kim wipe without disturbing the arranged embryos. A few drops of DPX were used when imaging was done with Olympus Fluoview 10i. SlowFade Gold solution was added in the case of Leica TCS SP8 confocal microscopy. A coverslip was placed carefully on top without forming any air bubbles, and the edges were sealed using transparent nail polish. The slides were stored in a slide box at 4^{o}C until it is taken for imaging.

2.13 Image acquisition

Embryos stained for pAMPK, tAMPK, tubulin, phalloidin are done using Olympus Fluoview 10i under 63X water immersion objective. The numerical aperture was set to 2. Z stack size was system optimised to 0.4. Embryos stained for streptavidin and polarity markers including E cad, Dlg, Sqh and phalloidin are done using Leica confocal SP8 under 63X oil immersion objective. The numerical aperture was set to 1. Z stack size was system optimised to 0.3.

Live imaging using Leica confocal SP8 microscope under 63X oil immersion. F1 embryos from tGPH PIP3 Gal4 crossed with AMPK RNAi is used for looking at the early syncytial from NC11 to NC13. Z stack was system optimised to 1.5 range. The airy unit was set to 2. Laser power was set to 1.5.

2.14 Image analysis

All quantifications were performed using Fiji (ImageJ). Temporal information for live imaging movies was extracted using the Zen Lite software and LAS X. For measuring cap areas in live movies/fixed images, the apical-most section where caps are visible was chosen for each time frame of interest. A region of interest (ROI) was drawn along the perimeter of each selected cap using the polygonal selection tool, and the area was measured. For measuring pseudocleavage furrow lengths in live imaging movies, an orthogonal view of the Z-stack obtained for each time frame of interest was obtained, an ROI was drawn on each selected furrow using the segmented line tool, and the length was measured. To measure the contractile ring area, the basal most plane of furrow progression was taken (each stage with corresponding furrow lengths and of equal depth). An ROI is drawn using a polygonal tool and area is measured. All the graphs were plotted and analyzed in GraphPad Prism 8.4.3.

CHAPTER 3: RESULTS AND DISCUSSION

3.1 The active form of AMPK shows dynamic localization during the syncytial blastoderm stage of embryonic development

Mitosis is a highly energy-intensive process crucial for accurate chromosome segregation, particularly notable in the rapid and synchronous cell divisions characteristic of *Drosophila* embryonic development until the cellularization stage. Therefore, investigating the role of AMPK, a key regulator of energy homeostasis, holds significant importance during these cell cycle stages. AMPK, in its active form, localizes to the mitotic apparatus, spanning from centrosomes to the spindle midzone throughout mitotic progression in the mammalian cell line (Vazquez-Martin et al., 2009). One of its critical functions is the regulation of mitotic spindle orientation, achieved through the phosphorylation of the myosin regulatory light chain (MRLC) (Thaiparambil et al., 2012). In mammalian cells, the specific activation of the AMPKα2 isoform plays a pivotal role in ensuring error-free chromosomal segregation. This process involves sequential phosphorylation events by CDK1 and PLK1, leading to the activation and function of AMPKα2 in orchestrating genomic stability during mitosis (Lu et al., 2021).

In mammalian cells, the active form of AMPK (phosphorylated AMPK or pAMPK) exhibits distinct localization patterns during mitotic progression. During prophase, pAMPK is observed to colocalize with the centrosome, appearing centrally within the nucleus. As the cell progresses into metaphase, pAMPK forms punctate structures at the spindle poles. Upon transition to anaphase, as the nucleus begins to migrate towards opposite poles, pAMPK localizes at the metaphase plate. Finally, during telophase, pAMPK consolidates into a single punctum at the center (Lu et al., 2021).

In *Drosophila* embryonic development, specifically during the syncytial stage (NC12), where rapid nuclear divisions take place, we wanted to explore the localisation of active AMPK. To this end we harvested embryos laid by Canton S flies for 3 hours and immunostained them for pAMPK. We observed similar patterns of pAMPK localization, albeit with some variations. During prophase, pAMPK puncta are present at opposite spindle poles. As the cell enters metaphase, pAMPK is localized both at the opposite poles and partially distributed at the metaphase plate on the nucleus (**Figure 3.1 a, b** white arrowhead). We assume this could be because the nuclear divisions occur more rapidly unlike in mammalian cells leaving some of the active AMPK at the spindle pole ready for the next division. During anaphase, pAMPK concentrates at the metaphase plate. Finally, at the end of telophase, pAMPK puncta are present at both nuclei following division (**Figure 3.1 a, b**). These observations corroborate with existing literature on dynamic localization of pAMPK in mammalian cell lines and suggest for the

first time that AMPK must have a conserved role in governing the energy-intensive syncytial cycles of *Drosophila* embryonic development.

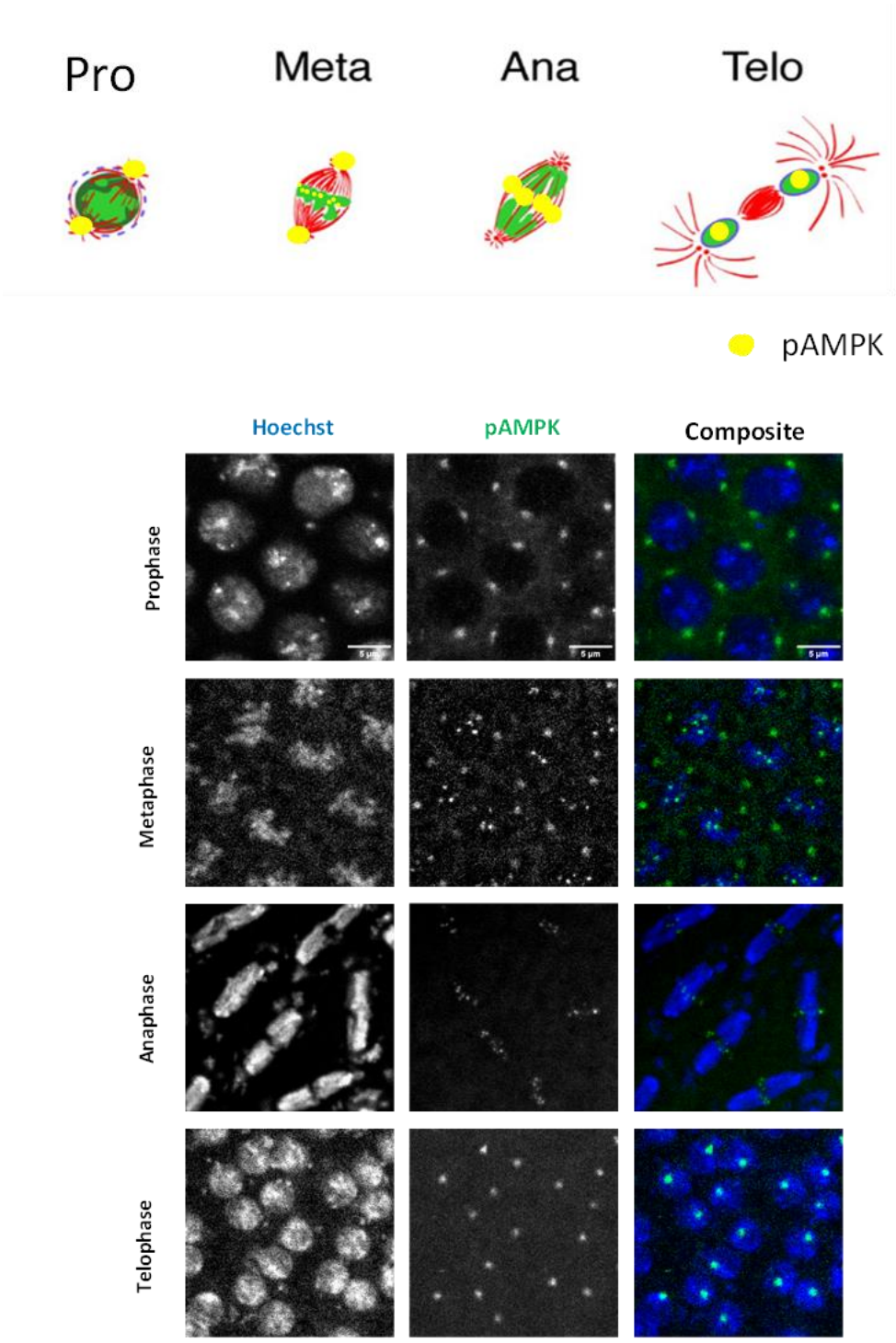

Fig 3.1 a) Schematic representation of different stages of mitosis starting from prophase, metaphase, anaphase, and telophase. The nucleus is marked in green; tubulin is marked in red, and pAMPK (active form of AMPK) is marked in yellow. b) Immunostaining of *Drosophila* embryo at NC 12 stage with nucleus stained in Heochst (Blue) and pAMPK stained in green. Each row signifies each stage of cell cycle division progression. White arrowheads represent pAMPK double localization at the metaphase stage. The scale bar represents 5µm. Imaging was done in Olympus Fluoview FV 10i. 5 to 6 embryos show similar phenotypes for each stage except 2 for telophase.

3.2 The effect of AMPK knockdown on embryonic lethality and egg laying capacity.

In order to study the effect of AMPK knockdown on embryonic lethality and egg laying capacity we opted for the GAL4-UAS system. The Gal4/UAS system is used to drive our gene's expression of interest in stage-specific patterns (Osterwalder et al., 2001). The stage-specific Gal4 driver line we used to understand the role of AMPK in early embryonic development was Nanos-Gal4. Nanos is a maternal gene that is expressed during oogenesis as well as during early embryo development (Wang et al.,1994). The Nanos-Gal4 driver specificity was confirmed by crossing it with the UAS-GFP line, where fluorescence was observed only in the abdomen of the F1 generation female fly and the embryo of the F2 generation as compared to control cross (**Figure 3.1 a**). The knockdown line we used for learning the role of AMPK by downregulation of AMPK in the early embryonic development was UAS-AMPK RNA^{i} transgenic line transfected with Valium 20 vector (BL #32371). The RNAi method uses shRNAs (small hairpin RNA) to knock down gene expression. We chose this line because Valium 20 gives more potent effects than VALIUM10 and works in the soma and the germline (Ni et al., 2010).

We confirmed whether the AMPK RNAi line used efficiently reduced AMPK levels using immunoblotting. The AMPK RNAi line used expresses dsRNA for RNAi of AMPK α, which is the AMPK catalytic subunit where the phosphorylation binding site is present, inhibiting the expression of AMPK α (Hardie, 2004). We observed a decrease in the protein level of phosphorylated AMPK (pAMPK) in the immunoblot fig.1B for AMPK knockdown flies compared to the control flies. Since it is a knockdown, we did not expect a complete reduction as some of the AMPK α will escape the knockdown and undergo translation (**Figure 3.1 b**). We did not observe much of a significant decrease in total AMPK protein level of AMPK knockdown embryos compared to control.

To further check the effect of AMPK knockdown on egg-laying capability and embryo viability, we used a Nanos-Gal4 driver to knock down AMPK during oogenesis and embryogenesis. To determine the impact on egg-laying ability, we performed an assay where F1 females (30) and males (10) from the experimental cross (Nanos-Gal4 * UAS AMPK RNA^{i}) and control cross (CS * UAS AMPK RNA^{i}) were allowed to mate in egg laying cage. The number of eggs laid in 6 and 12 hours were manually counted under the stereoscope. We observed a significant reduction in the egg-laying capability of AMPK knock-down flies (**Figure 3.1 e, e'**). Additionally, to address whether the AMPK knockdown affected the embryo viability, we observed 100 embryos laid by F1 flies (experimental cross and control) over 3 hours, arranged in a fresh agar plate for 24 hours. We manually counted hatched and unhatched embryos to quantify the viability after 24 hours. We observed a significant reduction in the embryo viability of the

AMPK knockdown flies compared to the control (**Figure 3.1 d**). Collectively, these data suggest that AMPK knockdown affects both egg laying and embryo viability.

Since the nanos-Gal4 driver line was also expressed during oogenesis for the continued production of egg chambers, we expected AMPK knockdown during that stage to affect the egg-laying capacity of the knockdown flies. Studies are proving the role of AMPK in multiple cell types of *Drosophila* ovaries, in both energy dependent and independent roles for example even basal amount is required for germline stem cells (GSC) maintenance in well-fed flies (Kaitlin et al., 2016).

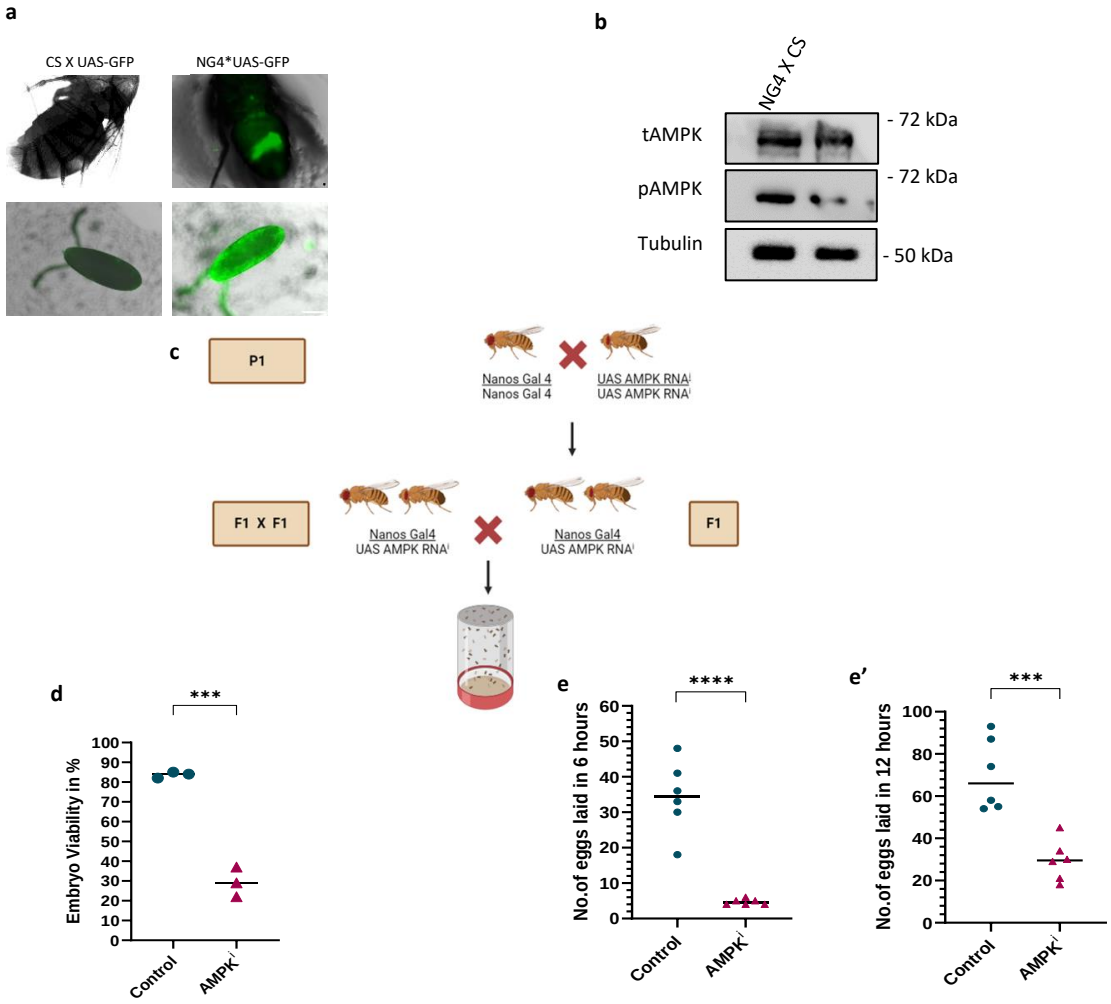

Fig 3.2 a) Driver line specificity was checked using UAS GFP line where green fluorescence is observed in the lower abdomen of F1 generation fly and F2 generation embryo (left panel of first and second row). b) An immunoblot assay was performed to check the knockdown effect on the NG4 X AMPKi line with the control. Tubulin was considered as the positive control. tAMPK protein expression was also checked on the same blot by stripping method. c) schematic representation of cross setup for the NG4 X AMPKi line. Experiments were done on F2 embryos laid by F1 self-crossed flies. d) Embryo viability in percentage calculated by the number of eggs hatched divided by the number of eggs placed multiplied by 100. n=100 embryos (the procedure repeated thrice on three). e) Egg laying after 6 hours and e') 12 hours, respectively. n=6 (6 different cage setups for each line). Student's T test ***p<0.001, ****p<0.0001

3.3 AMPK knockdown decrease furrow progression and increase sub-apical cap area during syncytial blastoderm stages of embryonic development

In AMPK mutant embryos, because of loss of active MRLC, disorganization in epithelial structure, abnormal genomic integrity, defective mitotic cells (polyploid chromosome), and abnormal cell polarity were observed in mammalian cells (Thaiparambil et al., 2012). AMPK also controls membrane lipid organization and outward phosphatidyl-Ser translocation (Ana et al., 2013). Thus AMPK plays a vital role in membrane organisation.

Knocking down of AMPK is expected to disrupt epithelial polarity proteins like actin and myosin (Munjal & Lecuit, 2014). Increased Myosin II contractility leads to shorter furrows since furrow ingression relies on lateral cap growth and buckling (Zhang et al., 2018). This can also result in a restriction on cap expansion during these stages. AMPK activation by pharmacological and genetic inhibition of ATP production by mitochondria has been shown to decrease syncytial stage embryo metaphase furrow extension (Chowdhary et al., 2017). Therefore, to investigate the effect of AMPK on membrane organisation during early embryonic development, we used a tGPH (tubulin–green fluorescent protein (GFP)–pleckstrin homology) line with maternal tubulin-Gal4 driver line crossed with AMPK RNAi to understand furrow progression and cap area by live imaging. These tGPH-expressing embryos are used mainly to study NC11 to NC13 stages of embryonic development towards understand membrane organisation. The embryos were collected in one hour and mounted for live imaging from NC11.

The apical cap area seems to be expanded for the AMPK knockdown embryo compared to the control line, and there was a consistent increase in this area for five embryos (**Figure 3.3 b**). This increase was seen during all the cell cycle stages, with a higher significant increase during metaphase and anaphase. This difference in the sub-apical area was more prominent during the NC13 stage than the NC12 stage. (**Figure 3.3 d**). The cap area does not seem to be affected by the knockdown. While the sub-apical area expanded, the furrow ingression seems to be reduced during these stages (**Figure 3.3 b**). The furrow ingression is significantly reduced during the metaphase and anaphase stages, which is higher than other stages, and the same is valid for area expansion (**Figure 3.3 c**). To summarize, knocking down AMPK seems to cause cap expansion with increased areas, leading to increased sub-apical area and inhibiting furrow ingression, which is consistent with our expectations, suggesting AMPK influences furrow ingression and contractile ring dynamics during the metaphase furrow extension during syncytial stages.

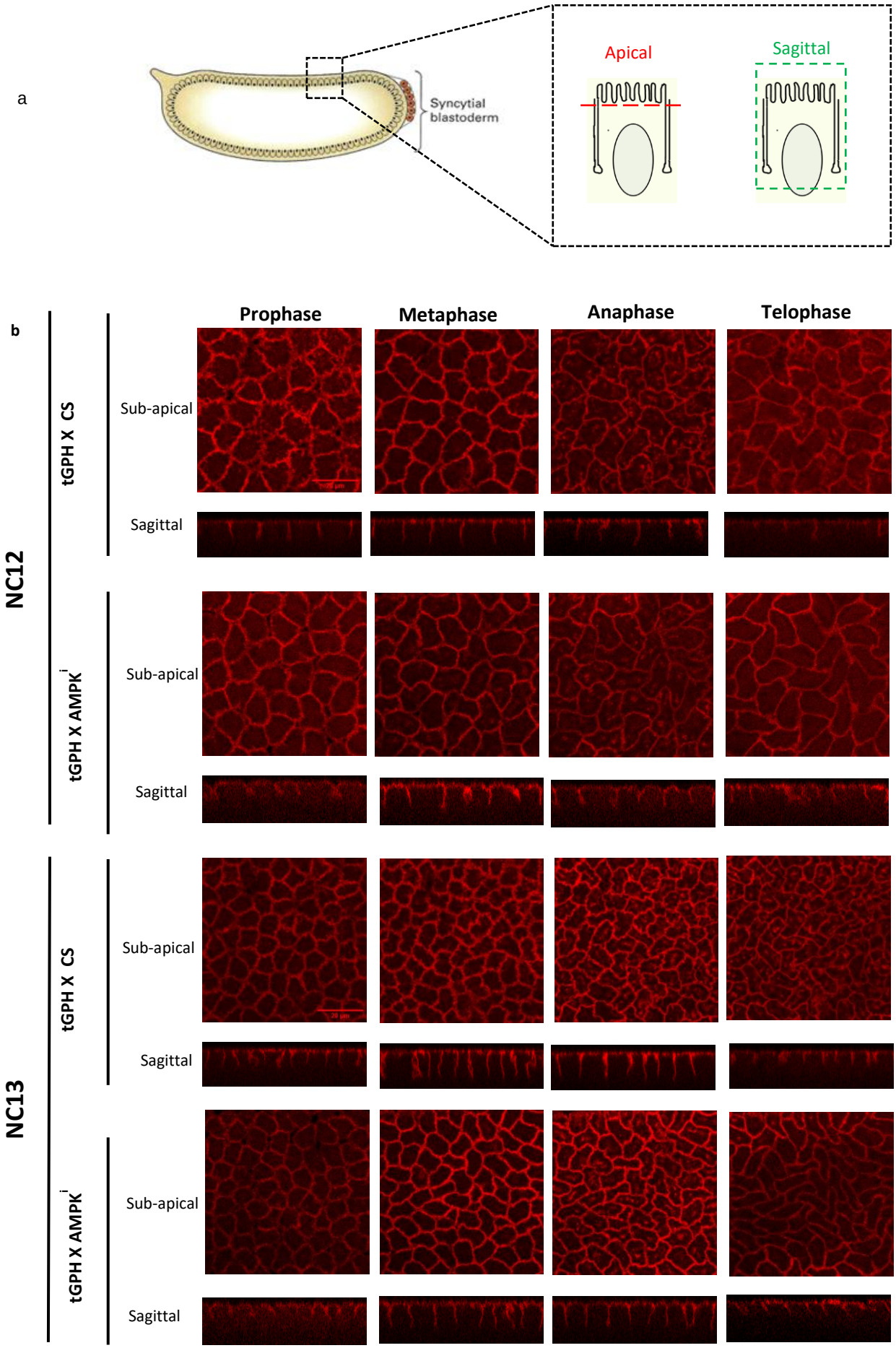
a
Syncytial blastoderm
Apical
Sagittal
b
Prophase
Metaphase
Anaphase
Telophase
NC12
tGPH X CS
Sub-apical
Sagittal
tGPH X AMPK^{i}
Sub-apical
Sagittal
NC13
tGPH X CS
Sub-apical
Sagittal
tGPH X AMPK^{i}
Sub-apical
Sagittal

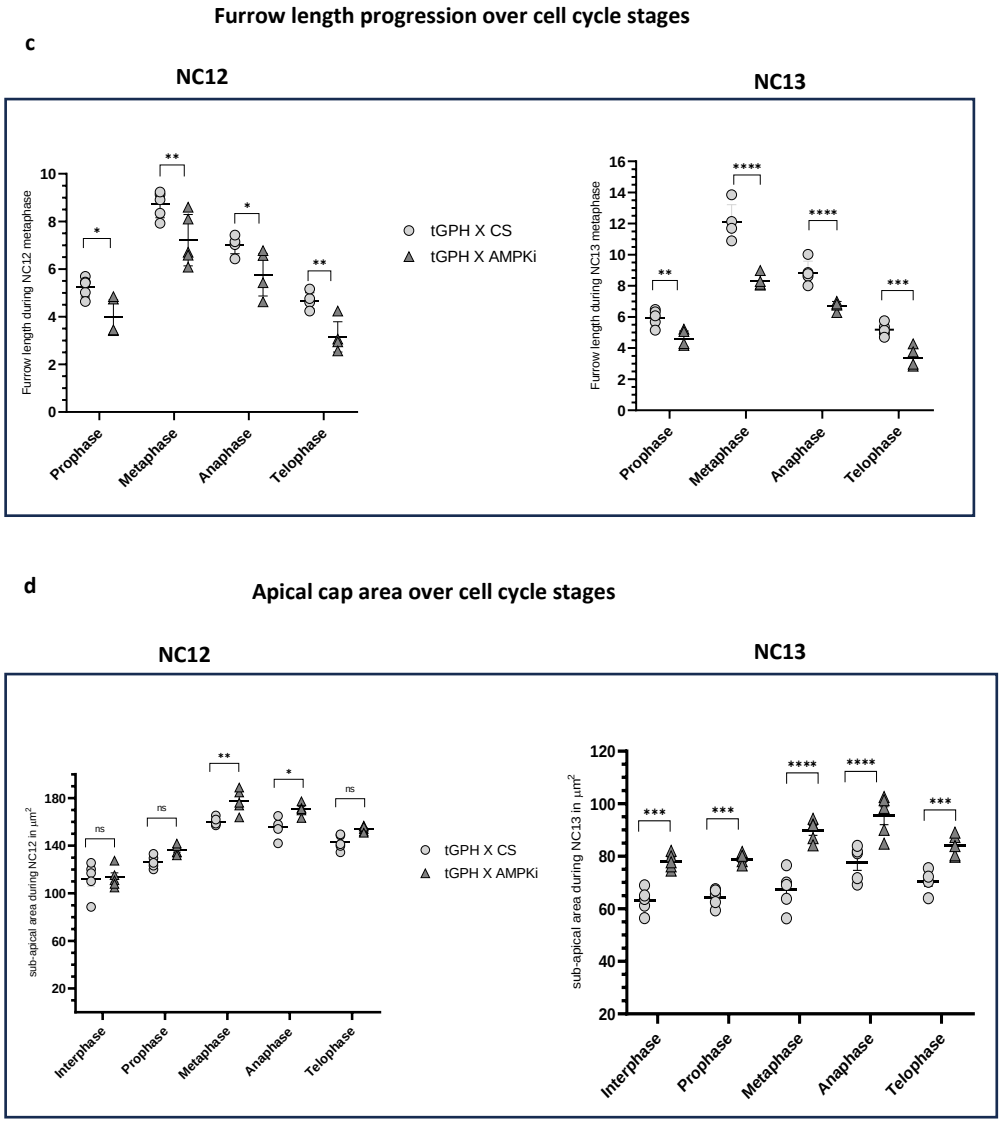

Fig 3.3 a) Schematic of syncytial *Drosophila* embryo depicting apical and orthogonal/sagittal sections of syncytial pseudo-cells studied from live imaging data. b) apical (xy) and orthogonal/sagittal (xz) snapshots from live imaging of tGPH-expressing control and AMPK RNAi embryos. The first two rows represent NC12, and the bottom two represent NC13 embryos. The scale bar represents 20 µm. c,d) . Quantification of furrow lengths and cap areas, respectively. Furrow length is quantified from prophase to telophase, and apical cap area is measured from interphase to telophase. n=5 embryos for both control and AMPK^{i}. 5-6 caps and 8-10 furrows per embryo calculated. Data is represented as mean ± s.d. ns, not significant; *, $p < 0.05$; **, $p < 0.01$; ***, $p < 0.001$; ****, $p < 0.0001$, 2way Anova Sidaks multiple comparisons test.

3.4 AMPK knockdown leads to hyper constriction of the contractile ring during the mid-cellularization stage of embryonic development

Drosophila cellularization happens through the elongation of the plasma membrane furrow between neighboring nuclei, which takes around 45 minutes at 25°C to go from 3 µm (early) to 40 µm (late) (Swati et al., 2021). Early in cellularization, the nuclei are spherical but elongate as the process progresses. In the early phases of cellularization, contractile ring construction begins near the base of the furrow tip, where Myosin II is recruited in foci within a polygonal network. Actomyosin-based contractile rings constrict and form more circular shapes during mid and late-stage cellularization at the base of elongated nuclei (Swati et al., 2021).

To assess the function of AMPK during this process, RNAi knockdown strategy is used to deplete the level of AMPK. This line was crossed to a maternal-Gal4 line (nanos-Gal4) to express shRNA during oogenesis and embryogenesis. Control and knockdown embryos collected after 3 hours of fertilization is stained with Phalloidin, which marks the cortical F-actin, and Streptavdidn, which marks the mitochondria. In control embryos, during the early stages of cellularization (furrow length 3–6 µm), a polygonal array was observed with F actin staining at the end of the furrow as expected. During the mid-cellularization stage (furrow length 6–16 µm) and late-cellularization stage (furrow length 16–40 µm), the polygonal architecture transitioned to circular with more constriction as the process progressed (**Figure 3.4 a**).

In the AMPK knockdown embryos, we observed enhanced constriction of the contractile ring during the mid and late stages of cellularization. During the mid-cellularization stage, this constriction is higher, and the furrow tip showing a teardrop shape seems to localize in the opposite direction (**Figure 3.4 c, d** white arrowhead). This phenotype was observed in four out of five embryos during this stage. Quantifying the contractile ring area during these stages also showed a significant reduction in the area for mid and late cellularisation stages compared to the control (**Figure 3.4 e**). We also observed no change in the presence of mitochondria in both control and AMPK knockdown conditions, showing that depleting AMPK does not affect the localization and number of mitochondria in the embryo apically and laterally (**Figure 3.4 b**)**.** All this shows that AMPK depletion leads to untimely and premature constriction of F-actin present at the furrow tip during the cellularization stage of embryonic development, leading to the role of AMPK in maintaining the furrow progression and ring constriction process over the stages.

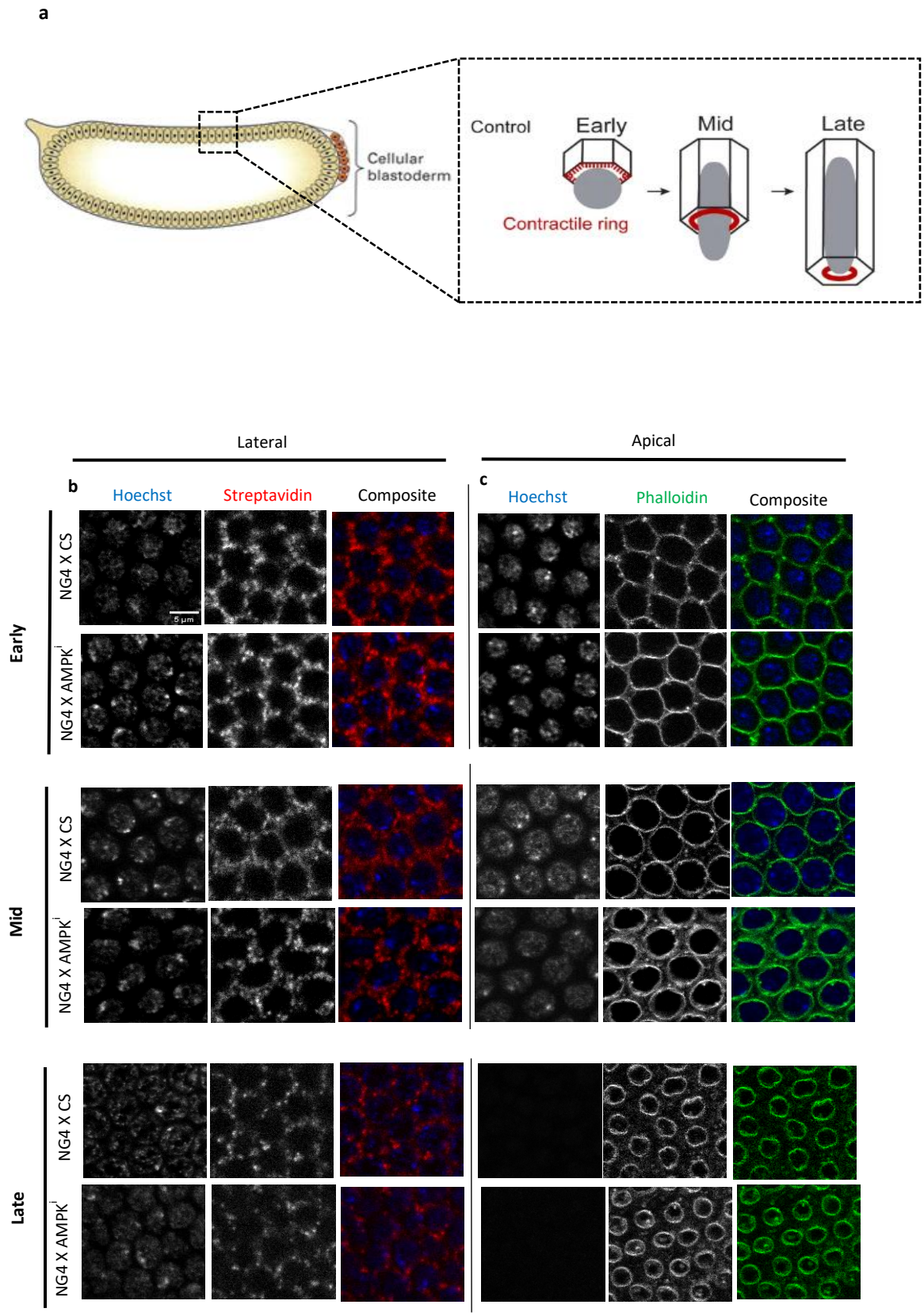
a
Cellular blastoderm
Control
Early
Mid
Late
Contractile ring
Lateral
Apical
b
Hoechst
Streptavidin
Composite
c
Hoechst
Phalloidin
Composite
Early
Mid
Late
NG4 X CS
NG4 X AMPK'
5 µm

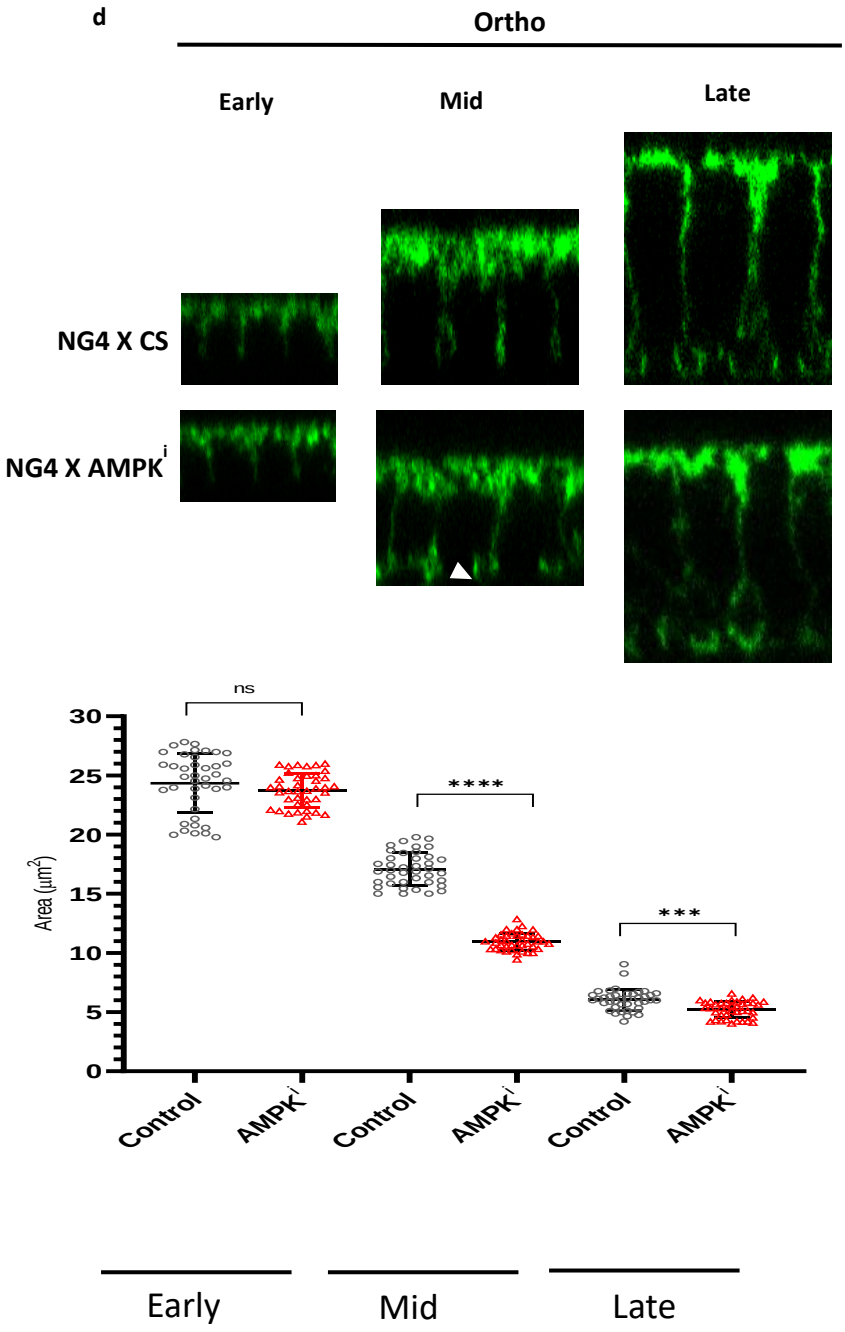

Fig 3.4 a) Schematic depiction of cellularization in the *Drosophila* embryo with plasma membrane (black), nuclei (gray), and contractile ring (red) organization at the base of the furrow. The furrow base where the contractile ring assembles is hexagonal at the early stage, circular at the mid-stage, and constricted at the late stage. Schematic adapted from (Swati et al., 2021). b) The image panel shows embryos in both the control and AMPK RNAi, immunostained with Streptavidin(red), Phalloidin (green), and Hoechst (blue). The first three rows show lateral streptavidin staining around the middle of furrow progression in each stage, and the next three rows show phalloidin staining at the furrow end. The scale bar represents 5 µm. d) Ortho (xz) view of phalloidin staining for the image panel above. The white arrowhead represents the teardrop furrow ends constricting more. e) Scatter plot shows the area of the ring in the control and AMPKi during early (3–6 µm furrow length), mid (6–16 µm), and late (16–40 µm) stages of cellularization (n = 40 rings, 10 per embryo, 4 embryos each). Data is represented as mean ± s.d. ns, not significant; *, $p < 0.05$; **, $p < 0.01$; ***, $p < 0.001$; ****, $p < 0.0001$, . two-tailed Mann–Whitney test.

3.5 AMPK knockdown leads to Myosin II enrichment at the contractile ring during the mid-cellularization stage and loss of epithelial integrity.

An early event of cellularization is the recruitment of non-muscle myosin II(Myosin II) to the basal tip of the progressing furrow. Myosin initially, during the early stage of cellularization, forms an interconnect polygonal basal array and later reorganizes to a cytokinetic ring and localizes at the contractile ring. AMPK has been shown to phosphorylate MRLC (Myosin regulatory chain) to regulate cell polarity and mitosis. Embryos from *AMPKα*-GLC epithelia revealed irregular distribution of various polarity markers such as Bazooka, β-catenin, and Discs-large throughout the epithelium (Lee et al., 2007).

We utilized the maternal driver line nanos-Gal4 crossed with AMK RNAi to investigate the impact of AMPK during the energy-driven cytokinesis event occurring in the cellularization stage of *Drosophila* embryo development. As embryonic development is an energy-demanding process, cellularization signifies the initial formation of epithelial cells, which is governed by polarity proteins. Myosin is localized at the leading edge of the advancing furrow during cellularization. Being part of the contractile ring, Myosin II also orchestrates the constriction of the furrow during the mid to late stages of cellularization.

To explore the role of myosin and polarity markers during this process, we conducted staining on embryos collected three hours post-fertilization from both control and AMPK knockdown groups. Specifically, we stained for spaghetti squash (sqh), which serves as the regulatory light chain of nonmuscle type 2 myosin, and Dlg (Disc large), a marker for lateral polarity junctions.

Our examination revealed a hyper-constriction of the contractile ring during the mid and later stages of cellularization in the embryos, as evidenced by quantifying the area of the ring based on F-actin staining. This phenotype was mirrored in the mid and later stages of cellularization when stained for Sqh. Interestingly, Sqh staining showed a denser localization of myosin surrounding the contractile ring area, forming a distinct thick band of myosin, particularly pronounced during the mid stage of cellularization. This phenotype was consistently observed in five out of six embryos stained for Sqh (**Figure 3.5 b**).

Furthermore, we noted an irregular distribution of Discs-large (Dlg), a marker for basolateral polarity, throughout the cells. Dlg was observed to be more abundant within the cell rather than at the lateral junctions during all three stages of cellularization (**Figure 3.5 c**). These observations can be summarized as follows: AMPK knockdown leads to Myosin II enrichment at the contractile ring during the mid-cellularization stage. Moreover, AMPK knockdown may also play a role in regulating epithelial integrity, as indicated by the irregular distribution of

Discs-large (Dlg) throughout all cellularization stages. This process is critical for forming the epithelial layer enveloping the embryo.

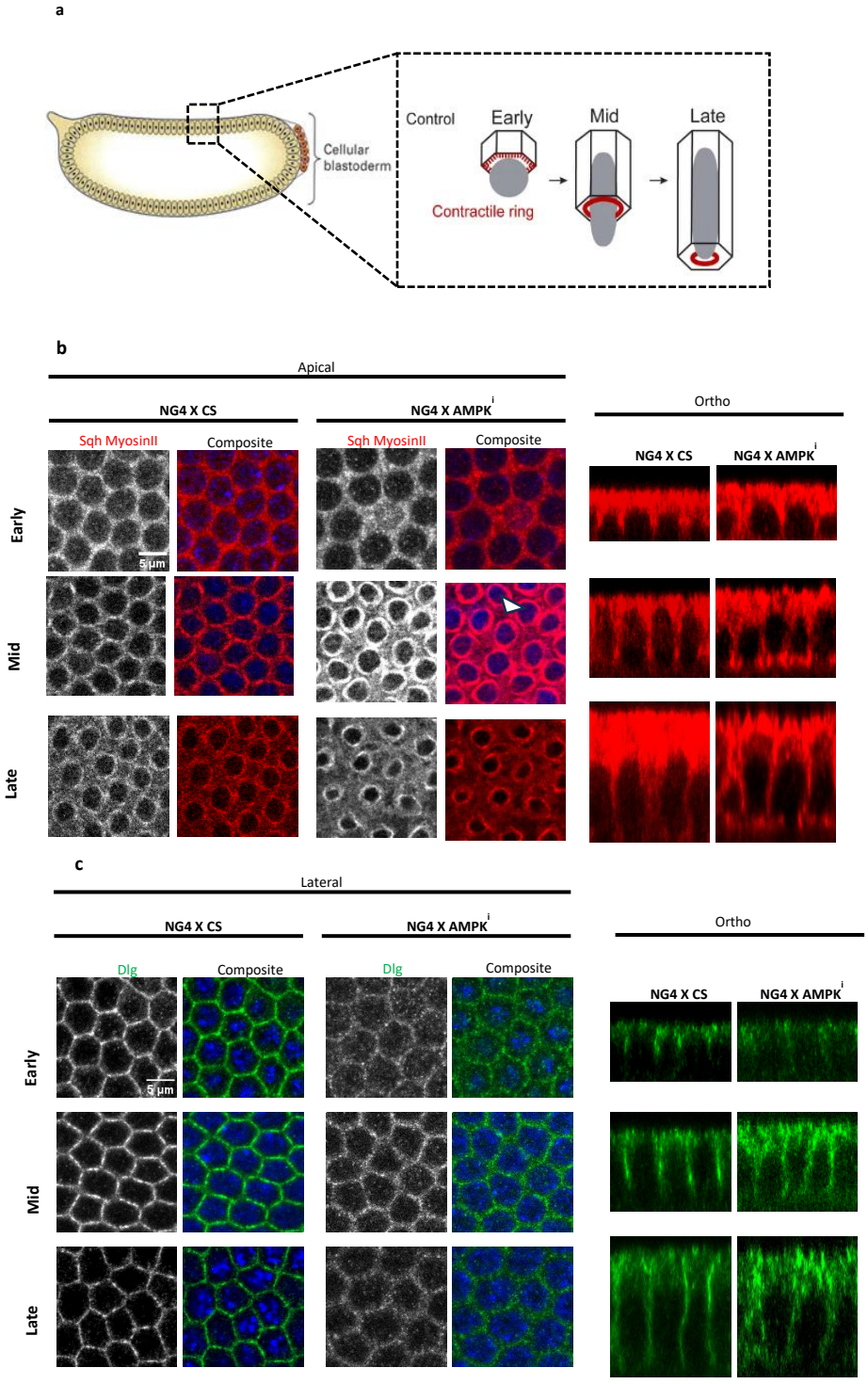

Fig 3.5 a) Schematic depiction of cellularization in the *Drosophila* embryo with plasma membrane (black), nuclei (gray), and contractile ring (red) organization at the base of the furrow. The furrow base where the contractile ring assembles is hexagonal at the early stage, circular at the mid-stage, and constricted at the late stage. Schematic

adapted from (Swati et al., 2021). b) Apical and orthogonal images of control embryos in the first two rows (composite image is with Hoechst), and the next two rows are AMPK knockdown embryos. The embryos are stained for sqh (red). The white arrowhead represents the thickening of the myosin band near the contractile ring area. c) Apical and orthogonal images of control embryos in the first two rows (composite image is with Hoechst), and the next two rows are AMPK knockdown embryos. The embryos are stained for dlg (green). The scale bar represents 5 μm.

CHAPTER 4 DISCUSSION

The role of AMPK during early embryonic development in *Drosophila* remains a relatively underexplored area of research. Given its pivotal role in maintaining energy homeostasis and its involvement in various physiological activities ranging from cell division, cell polarity establishment, genomic integrity maintenance, to chromosome segregation, there is a compelling rationale to investigate its functions during highly energy-sensitive and morphogenetic events occurring in early embryogenesis.

This study aims to elucidate the role of AMPK during both the syncytial blastoderm stage and the subsequent cellularization stage of *Drosophila* embryonic development. Our focus lies on investigating the dynamic localization patterns of active AMPK and how they differ from those observed in mammalian systems. Furthermore, we seek to understand how AMPK contributes to the regulation of membrane organization during these critical developmental stages. During syncytial blastoderm formation and cellularization, the embryo undergoes intricate changes including furrow extension, maintenance of the actomyosin network to facilitate contractile ring constriction, and establishment of polarity markers such as Dlg to ensure normal cellular growth.

Our approach involved perturbing AMPK expression using an AMPK RNAi line and observing any resultant phenotypic changes, particularly focusing on cellular morphological alterations during the syncytial blastoderm and cellularization stages of *Drosophila* embryonic development. Through our experiments, several key observations emerged.

One notable effect of AMPK knockdown was observed in the egg-laying capacity of the flies. By utilizing a maternal-Gal4 driver (nanos-Gal4), which is active during both oogenesis and embryogenesis, we were able to assess the impact of AMPK knockdown in the ovaries of F1 flies resulting from the cross. Significantly reduced egg production in the knockdown flies compared to control flies indicates the importance of AMPK during oogenesis or follicular development in *Drosophila*.

This finding aligns with the role of AMPK as a central regulator of energy homeostasis, which has been extensively studied in mammalian systems. In mammals, AMPK is closely associated with various aspects of female reproduction, including follicular development, granulosa cell proliferation, and pregnancy regulation (Yang et al., 2020). Therefore, investigating the role of AMPK in invertebrate systems such as *Drosophila* becomes crucial for understanding which factors are affected during the process of oogenesis. By elucidating the molecular mechanisms underlying AMPK's involvement in reproductive processes in *Drosophila*, we can gain valuable insights into its broader functions in developmental biology and reproductive health.

Numerous studies have provided evidence supporting the role of AMPK in controlling the cell cycle (Igata et al., 2005) and mitosis (Thaiparambil et al., 2012; Banko et al., 2011) through distinct mechanisms. Additionally, AMPK has been implicated in regulating the fidelity of chromosome segregation (Zhao et al., 2020) and maintaining genomic integrity (Lee et al., 2007). Therefore, examining the role of AMPK during the rapid and synchronous cell cycles occurring in early embryonic development can offer valuable insights into whether AMPK plays a significant role in these vital events.

In both mammalian cells and *Drosophila* embryonic development, the active form of AMPK (phosphorylated AMPK or pAMPK) demonstrates distinct localization patterns throughout mitotic progression. Notably, during prophase, pAMPK colocalizes with the centrosome in mammalian cells, whereas in *Drosophila* embryos at the syncytial stage (NC12), pAMPK puncta are observed at opposite spindle poles. This initial localization suggests a conserved role for AMPK in mitotic regulation across species. As mitosis progresses into metaphase, pAMPK exhibits specific localization changes. In mammalian cells, pAMPK forms punctate structures at the spindle poles during this stage, while in *Drosophila* embryos, pAMPK is doubly localized at opposite poles and partially distributed at the metaphase plate on the nucleus. This divergence in pAMPK localization between mammalian cells and *Drosophila* embryos may reflect species-specific regulatory mechanisms governing mitotic processes. During anaphase, a further variation in pAMPK localization is observed. In mammalian cells, pAMPK concentrates at the metaphase plate as the nucleus migrates towards opposite poles, whereas in *Drosophila* embryos, pAMPK remains concentrated at the metaphase plate during this stage. This discrepancy highlights potential differences in the timing or mechanisms of pAMPK regulation between mammalian and *Drosophila* mitosis. Finally, after telophase, pAMPK localization patterns exhibit dissimilarities between mammalian cells and *Drosophila* embryos. pAMPK puncta are present at both nuclei following division in *Drosophila*, while it is centrally located in the mammalian system. Since centrosomes are very closely present with

the nucleus and present apically, the appearance of pAMPK over the nucleus during the telophase stage can be a reason for the *Drosophila* embryo (Lu et al., 2017).

The distinct localization patterns of phosphorylated AMPK (pAMPK) observed during mitotic progression in both mammalian cells and *Drosophila* embryos highlight the significance of AMPK in regulating mitosis across different species. Understanding the involvement of AMPK in early embryonic development provides crucial knowledge about its potential contributions to fundamental cellular processes during this critical developmental stage. By elucidating the specific mechanisms by which AMPK influences mitosis and cell cycle progression, we can gain a deeper understanding of its broader functions in embryonic development and cellular physiology.

In our investigation of AMPK's role in membrane organization during embryonic development, we initially focused on the syncytial blastoderm stages. Actin dynamics play a crucial role in cortical divisions and metaphase furrow extension during this developmental phase. Actin is prominently present throughout furrow extension and membrane organization induced by centrosomes (Wiley et al., 2010). Notably, this coincides with the expansion of the apical actin cap, reaching its maximum extent during metaphase when furrow progression is at its peak, facilitating the separation between neighboring spindles.

In embryos subjected to AMPK knockdown, we observed a significant reduction in furrow length, indicating the impact of AMPK depletion on membrane organization during this stage. Furthermore, the cell area was found to be increased in AMPK knockdown embryos compared to controls. Furrow progression is crucial during cortical divisions, where nuclei divide within a tightly packed monolayer. Mutants disrupting furrow formation often exhibit fused spindles and abnormal nuclear divisions (Sullivan et al., 1993). The decreased furrow progression observed in AMPK knockdown embryos may lead to an increase in cell area, potentially facilitating progression through the cell cycle to the next stage. These observations suggest that AMPK plays a significant role in regulating membrane organization and furrow progression during syncytial blastoderm stages of embryonic development. Further investigations into the specific molecular mechanisms underlying AMPK's involvement in these processes will enhance our understanding of its role in embryogenesis and cellular dynamics.

In our investigation of AMPK's role in actomyosin dynamics during the cellularization stage of embryonic development, we observed a series of intricate processes crucial for cellular morphogenesis. During the cellularization stage of *Drosophila* embryonic development, a prolonged interphase is marked by a dynamic rearrangement of actomyosin dynamics. An actin-myosin ring is present at the leading edge of ingressing furrows, moving basally along the microtubule basket. Adherens junctions connect neighboring furrows, and upon

completion of furrow elongation, lateral furrow constriction occurs, known as basal closure, facilitated by contractile ring constriction. This process involves the contraction of filamentous actin networks by non-muscle myosin II, which generates force during cell and tissue morphogenesis (Munjal & Lecuit, 2014; Martin & Goldstein, 2014). As furrow ingression proceeds, the actomyosin network reorganizes into individual actomyosin rings, which constrict to close the basal side of newly formed cells, resembling animal cytokinesis (Schejter & Wieschaus, 1993). Notably, several proteins involved in cytokinesis, including Scraps (Anillin homolog), Septins, Rho1 (RhoA homolog), and Diaphanous (Dia), also function in cellularization (Field et al., 2005; Adam et al., 2000; Crawford et al., 1998; Afshar et al., 2000; Grosshans et al., 2005).

AMPK, known for its role in matching cell cycle progression to energy availability, is proposed to regulate cell polarity, mitotic progression, and cytokinesis (Vasquez et al., 2007). Studies in *Drosophila melanogaster* have highlighted the importance of AMPK in cytokinesis and cell proliferation. Mutation of the α-catalytic subunit of AMPK led to disruptions in cell polarity and enhanced cell proliferation under metabolic stress (Mirouse et al., 2007). AMPK-null germ-line clones exhibited gross mitotic defects, including lagging chromosomes, failure to complete cytokinesis, polyploidy, and embryonic lethality. AMPK has been shown to phosphorylate the non-muscle myosin regulatory light chain (MRLC; also known as MRLC2) on Ser22, facilitating changes in the actin cytoskeleton essential for maintaining cell polarity (Lee et al., 2007).

In AMPK knockdown embryos, we observed a hyper constriction during the mid stage of cellularization was observed, coinciding with a thick band of myosin around the contractile ring edge. Given AMPK's role in regulating MRLC, reduced AMPK levels may dysregulate MRLCII phosphorylation, leading to increased myosin production in that area. This phenotype, predominant at the mid stage of cellularization, became less significant or more normalized at the late stage, suggesting a spatial and temporal regulation of myosin levels mediated by AMPK knockdown.

Further investigations into the effects of AMPK knockdown during early embryonic stages, particularly focusing on membrane organization and cell polarity, could provide valuable insights. Utilizing an AMPK overexpression line would enable us to discern whether observed phenotypes are altered. Additionally, studying chromosome organization during each stage with reduced AMPK levels would shed light on its role in this development aspect. Also the connection between AMPK and MRLC for maintain cell polarity, actin-myosin interactions and its production and its role in regulating cytokinesis during the early embryonic development of *Drosophila* can be interpreted better by looking more into it.

AMPK has been implicated as both a tumor suppressor during cancer initiation and a promoter of metastasis once cancer has initiated. Since epithelial-mesenchymal transition (EMT) occurs during metastasis in cancer and gastrulation in development, exploring the role of AMPK during this process could elucidate how AMPK contributes to cancer progression. Understanding how AMPK operates in EMT, a process cancer hijacks from early development for its own benefit, could offer insights into potential therapeutic interventions targeting AMPK in cancer treatment, especially during metastasis.

REFERENCES

Banko, M. R., Allen, J. J., Schaffer, B. E., Wilker, E. W., Tsou, P., White, J. L., ... & Brunet, A. (2011). Chemical genetic screen for AMPKα2 substrates uncovers a network of proteins involved in mitosis. Molecular cell, 44(6), 878-892.

Bashirullah, A., Halsell, S. R., Cooperstock, R. L., Kloc, M., Karaiskakis, A., Fisher, W. W., ... & Lipshitz, H. D. (1999). Joint action of two RNA degradation pathways controls the timing of maternal transcript elimination at the midblastula transition in Drosophila melanogaster. The EMBO journal, 18(9), 2610-2620.

Cantrell, D. A. (2019). Move to metabolism. Nature Reviews Immunology, 19(5), 270-270.

Castanon, I., & Baylies, M. K. (2002). A Twist in fate: evolutionary comparison of Twist structure and function. Gene, 287(1-2), 11-22.

Chen, L., Wang, J., Zhang, Y. Y., Yan, S. F., Neumann, D., Schlattner, U., ... & Wu, J. W. (2012). AMP-activated protein kinase undergoes nucleotide-dependent conformational changes. Nature structural & molecular biology, 19(7), 716-718.

Chowdhary, S., Tomer, D., Dubal, D., Sambre, D., & Rikhy, R. (2017). Analysis of mitochondrial organization and function in the Drosophila blastoderm embryo. Scientific reports, 7(1), 5502.

Chowdhary, S., Tomer, D., Dubal, D., Sambre, D., & Rikhy, R. (2017). Analysis of mitochondrial organization and function in the Drosophila blastoderm embryo. Scientific reports, 7(1), 5502.

Edgar, B. A., & O'Farrell, P. H. (1989). Genetic control of cell division patterns in the Drosophila embryo. Cell, 57(1), 177-187.

Foe, V. E. (1989). Mitotic domains reveal early commitment of cells in Drosophila embryos. Development, 107(1), 1-22.

Fogarty, S., Ross, F. A., Vara Ciruelos, D., Gray, A., Gowans, G. J., & Hardie, D. G. (2016). AMPK causes cell cycle arrest in LKB1-deficient cells via activation of CAMKK2. Molecular Cancer Research, 14(8), 683-695.

Frescas, D., Mavrakis, M., Lorenz, H., DeLotto, R., & Lippincott-Schwartz, J. (2006). The secretory membrane system in the Drosophila syncytial blastoderm embryo exists as

functionally compartmentalized units around individual nuclei. The Journal of cell biology, 173(2), 219-230.

Gowans, G. J., Hawley, S. A., Ross, F. A., & Hardie, D. G. (2013). AMP is a true physiological regulator of AMP-activated protein kinase by both allosteric activation and enhancing net phosphorylation. Cell metabolism, 18(4), 556-566.

Gracia, M., Theis, S., Proag, A., Gay, G., Benassayag, C., & Suzanne, M. (2019). Mechanical impact of epithelial-mesenchymal transition on epithelial morphogenesis in Drosophila. Nature communications, 10(1), 2951.

Hardie, D. G. (2004). The AMP-activated protein kinase pathway–new players upstream and downstream. Journal of cell science, 117(23), 5479-5487.

Hawley, S. A., Boudeau, J., Reid, J. L., Mustard, K. J., Udd, L., Mäkelä, T. P., ... & Hardie, D. G. (2003). Complexes between the LKB1 tumor suppressor, STRADα/β and MO25α/β are upstream kinases in the AMP-activated protein kinase cascade. Journal of biology, 2, 1-16.

Hawley, S. A., Ross, F. A., Gowans, G. J., Tibarewal, P., Leslie, N. R., & Hardie, D. G. (2014). Phosphorylation by Akt within the ST loop of AMPK-α1 down-regulates its activation in tumour cells. Biochemical Journal, 459(2), 275-287.

He, B., Martin, A., & Wieschaus, E. (2016). Flow-dependent myosin recruitment during Drosophila cellularization requires zygotic dunk activity. Development, 143(13), 2417-2430.

Iseli, T. J., Walter, M., van Denderen, B. J., Katsis, F., Witters, L. A., Kemp, B. E., ... & Stapleton, D. (2005). AMP-activated protein kinase β subunit tethers α and γ subunits via its C-terminal sequence (186–270). Journal of Biological Chemistry, 280(14), 13395-13400.

Jaleel, M., McBride, A., Lizcano, J. M., Deak, M., Toth, R., Morrice, N. A., & Alessi, D. R. (2005). Identification of the sucrose non-fermenting related kinase SNRK, as a novel LKB1 substrate. FEBS letters, 579(6), 1417-1423.

Ji, H., Ramsey, M. R., Hayes, D. N., Fan, C., McNamara, K., Kozlowski, P., ... & Wong, K. K. (2007). LKB1 modulates lung cancer differentiation and metastasis. Nature, 448(7155), 807-810.

Johnson, E. C., Kazgan, N., Bretz, C. A., Forsberg, L. J., Hector, C. E., Worthen, R. J., ... & Brenman, J. E. (2010). Altered metabolism and persistent starvation behaviors caused by reduced AMPK function in Drosophila. PloS one, 5(9), e12799.

Jukam, D., Shariati, S. A. M., & Skotheim, J. M. (2017). Zygotic genome activation in vertebrates. Developmental cell, 42(4), 316-332.

Kang, Y., & Massagué, J. (2004). Epithelial-mesenchymal transitions: twist in development and metastasis. Cell, 118(3), 277-279.

Kazgan, N., Williams, T., Forsberg, L. J., & Brenman, J. E. (2010). Identification of a nuclear export signal in the catalytic subunit of AMP-activated protein kinase. Molecular biology of the cell, 21(19), 3433-3442.

Kishton, R. J., Barnes, C. E., Nichols, A. G., Cohen, S., Gerriets, V. A., Siska, P. J., ... & Rathmell, J. C. (2016). AMPK is essential to balance glycolysis and mitochondrial metabolism to control T-ALL cell stress and survival. Cell metabolism, 23(4), 649-662.

Laws, K. M., & Drummond-Barbosa, D. (2016). AMP-activated protein kinase has diet-dependent and-independent roles in Drosophila oogenesis. Developmental biology, 420(1), 90-99.

Lee, J. H., Koh, H., Kim, M., Kim, Y., Lee, S. Y., Karess, R. E., ... & Chung, J. (2007). Energy-dependent regulation of cell structure by AMP-activated protein kinase. Nature, 447(7147), 1017-1020.

Liang, J., & Mills, G. B. (2013). AMPK: a contextual oncogene or tumor suppressor?. Cancer research, 73(10), 2929-2935.

Lizcano, J. M., Göransson, O., Toth, R., Deak, M., Morrice, N. A., Boudeau, J., ... & Alessi, D. R. (2004). LKB1 is a master kinase that activates 13 kinases of the AMPK subfamily, including MARK/PAR-1. The EMBO journal, 23(4), 833-843.

Lott, S. E., Villalta, J. E., Schroth, G. P., Luo, S., Tonkin, L. A., & Eisen, M. B. (2011). Noncanonical compensation of zygotic X transcription in early Drosophila melanogaster development revealed through single-embryo RNA-seq. PLoS biology, 9(2), e1000590.

Lu, J., Huang, Y., Zhan, L., Wang, M., Xu, L., Mullen, M., ... & Yao, X. (2021). AMPKα2 activation by an energy-independent signal ensures chromosomal stability during mitosis. IScience, 24(4).

Mihaylova, M. M., & Shaw, R. J. (2011). The AMPK signalling pathway coordinates cell growth, autophagy and metabolism. Nature cell biology, 13(9), 1016-1023.

Miranda, L., Carpentier, S., Platek, A., Hussain, N., Gueuning, M. A., Vertommen, D., ... & Horman, S. (2010). AMP-activated protein kinase induces actin cytoskeleton reorganization in epithelial cells. Biochemical and biophysical research communications, 396(3), 656-661.

Neumann, D. (2018). Is TAK1 a direct upstream kinase of AMPK?. International journal of molecular sciences, 19(8), 2412.

Noto, H., Goto, A., Tsujimoto, T., & Noda, M. (2012). Cancer risk in diabetic patients treated with metformin: a systematic review and meta-analysis. PloS one, 7(3), e33411.

Pálfy, M., Joseph, S. R., & Vastenhouw, N. L. (2017). The timing of zygotic genome activation. Current opinion in genetics & development, 43, 53-60.

Pan, D. A., & Hardie, D. G. (2002). A homologue of AMP-activated protein kinase in Drosophila melanogaster is sensitive to AMP and is activated by ATP depletion. Biochemical Journal, 367(1), 179-186.

Pineda, C. T., Ramanathan, S., Tacer, K. F., Weon, J. L., Potts, M. B., Ou, Y. H., ... & Potts, P. R. (2015). Degradation of AMPK by a cancer-specific ubiquitin ligase. Cell, 160(4), 715-728.

Polyak, K., & Weinberg, R. A. (2009). Transitions between epithelial and mesenchymal states: acquisition of malignant and stem cell traits. Nature Reviews Cancer, 9(4), 265-273.

Polyak, K., & Weinberg, R. A. (2009). Transitions between epithelial and mesenchymal states: acquisition of malignant and stem cell traits. Nature Reviews Cancer, 9(4), 265-273.

Rabinowitz, M. (1941). Studies on the cytology and early embryology of the egg of Drosophila melanogaster. Journal of Morphology, 69(1), 1-49.

Rosivatz, E., Becker, I., Specht, K., Fricke, E., Luber, B., Busch, R., ... & Becker, K. F. (2002). Differential expression of the epithelial-mesenchymal transition regulators snail, SIP1, and twist in gastric cancer. The American journal of pathology, 161(5), 1881-1891.

Saxena, M., Balaji, S. A., Deshpande, N., Ranganathan, S., Pillai, D. M., Hindupur, S. K., & Rangarajan, A. (2018). AMP-activated protein kinase promotes epithelial-mesenchymal transition in cancer cells through Twist1 upregulation. Journal of cell science, 131(14), jcs208314.

Seher, T. C., & Leptin, M. (2000). Tribbles, a cell-cycle brake that coordinates proliferation and morphogenesis during Drosophila gastrulation. Current Biology, 10(11), 623-629.

Sharma, A., Anand, S. K., Singh, N., Dwivedi, U. N., & Kakkar, P. (2023). AMP-activated protein kinase: An energy sensor and survival mechanism in the reinstatement of metabolic homeostasis. Experimental Cell Research, 113614.

Sinnett, S. E., & Brenman, J. E. (2016). The Role of AMPK in Drosophila melanogaster. AMP-activated Protein Kinase, 389-401.

Swati Sharma, Richa Rikhy (2021). Spatiotemporal recruitment of RhoGTPase protein GRAF inhibits actomyosin ring constriction in Drosophila cellularization. eLife, 10, 63535

Tam, S. Y., Wu, V. W., & Law, H. K. (2020). Hypoxia-induced epithelial-mesenchymal transition in cancers: HIF-1α and beyond. Frontiers in oncology, 10, 486.

Tepass, U., Truong, K., Godt, D., Ikura, M., & Peifer, M. (2000). Cadherins in embryonic and neural morphogenesis. Nature reviews Molecular cell biology, 1(2), 91-100.

Thaiparambil, J. T., Eggers, C. M., & Marcus, A. I. (2012). AMPK regulates mitotic spindle orientation through phosphorylation of myosin regulatory light chain. Molecular and cellular biology, 32(16), 3203-3217.

Thiery, J. P. (2002). Epithelial–mesenchymal transitions in tumour progression. Nature reviews cancer, 2(6), 442-454.

Vazquez-Martin, A., Oliveras-Ferraros, C., & Menendez, J. A. (2009). The active form of the metabolic sensor AMP-activated protein kinase α (AMPKα) directly binds the mitotic apparatus and travels from entrosomes to the spindle midzone during mitosis and cytokinesis. *Cell cycle*, *8*(15), 2385-2398.

Vara-Ciruelos, D., Dandapani, M., & Hardie, D. G. (2020). AMP-activated protein kinase: Friend or foe in cancer?. Annual Review of Cancer Biology, 4, 1-16.

Vila, I. K., Yao, Y., Kim, G., Xia, W., Kim, H., Kim, S. J., ... & Song, M. S. (2017). A UBE2O-AMPKα2 axis that promotes tumor initiation and progression offers opportunities for therapy. Cancer cell, 31(2), 208-224.

Vila, I. K., Yao, Y., Kim, G., Xia, W., Kim, H., Kim, S. J., ... & Song, M. S. (2017). A UBE2O-AMPKα2 axis that promotes tumor initiation and progression offers opportunities for therapy. Cancer cell, 31(2), 208-224.

Winklbauer, R., & Müller, H. A. J. (2011). Mesoderm layer formation in Xenopus and Drosophila gastrulation. Physical biology, 8(4), 045001.

Wu, J., Rowart, P., Jouret, F., Gassaway, B. M., Rajendran, V., Rinehart, J., & Caplan, M. J. (2020). Mechanisms involved in AMPK-mediated deposition of tight junction components to the plasma membrane. American Journal of Physiology-Cell Physiology, 318(3), C486-C501.

Yang, J., Mani, S. A., Donaher, J. L., Ramaswamy, S., Itzykson, R. A., Come, C., ... & Weinberg, R. A. (2004). Twist, a master regulator of morphogenesis, plays an essential role in tumor metastasis. cell, 117(7), 927-939.

Yang, J., Mani, S. A., Donaher, J. L., Ramaswamy, S., Itzykson, R. A., Come, C., ... & Weinberg, R. A. (2004). Twist, a master regulator of morphogenesis, plays an essential role in tumor metastasis. cell, 117(7), 927-939.

Zheng, B., & Cantley, L. C. (2007). Regulation of epithelial tight junction assembly and disassembly by AMP-activated protein kinase. Proceedings of the National Academy of Sciences, 104(3), 819-822.